NASA TN D-1724

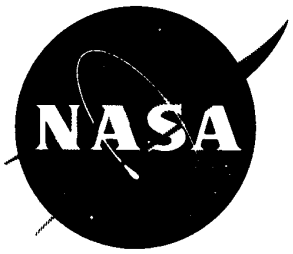

TECHNICAL NOTE

D-1724

CALIBRATIONS AND COMPARISONS OF PRESSURE-TYPE AIRSPEED-ALTITUDE SYSTEMS OF THE X-15 AIRPLANE FROM SUBSONIC TO HIGH SUPERSONIC SPEEDS

By Terry J. Larson and Lannie D. Webb

Flight Research Center
Edwards, Calif.

AUTHOR'S PERSONAL COPY

NATIONAL AERONAUTICS AND SPACE ADMINISTRATION

WASHINGTON

February 1963

NATIONAL AERONAUTICS AND SPACE ADMINISTRATION

TECHNICAL NOTE D-1724

CALIBRATIONS AND COMPARISONS OF PRESSURE-TYPE AIRSPEED-ALTITUDE SYSTEMS OF THE X-15 AIRPLANE FROM SUBSONIC TO HIGH SUPERSONIC SPEEDS

By Terry J. Larson and Lannie D. Webb

SUMMARY

Flight calibration data obtained from radar and rawinsonde balloon measurements to define position error are presented for static pressures sensed by a standard NACA pitot-static tube attached to a nose boom and a fuselage nose flush static system. The data for the two systems are compared from low subsonic speeds to 3.31, the highest comparable Mach number. Flight calibration data for subsonic and supersonic speeds are also presented and discussed for a pitot probe ahead of the canopy of the X-15.

Stagnation pressures from the pitot probe were found to be very sensitive to angle of attack above a Mach number of 1.8, since the probe is not located ahead of the aircraft bow wave. Above the transonic region, the Mach number and pressure-altitude errors resulting from nose-boom static-pressure errors increased with Mach number. At a Mach number of 3.31 (the highest Mach number attained with the nose-boom installation) the absolute Mach number error was 0.18, and the absolute pressure-altitude error was 2,200 feet. Although the nose-boom errors were relatively independent of angle of attack up to 12°, the flush static errors were significantly dependent on angle of attack as evidenced by the corresponding absolute Mach number and pressure-altitude errors resulting from this system at a Mach number of 3.31. At zero angle of attack the error was 0.88 in Mach number and 12,400 feet in pressure altitude; whereas, at an angle of attack of 12° the errors were, respectively, 0.50 and 6,300 feet. Similar to the nose-boom installation above the transonic region, the Mach number and pressure-altitude errors of the flush static system increased with Mach number. The errors at a Mach number of 4.0 for an angle of attack of 0° resulted in Mach number and pressure-altitude errors of 1.25 and 15,200 feet, respectively.

This study indicated that a nose-boom static-pressure installation is more suitable from the standpoint of position error and ease of calibration than a flush static system in the speed range from low subsonic to the highest Mach number (3.31) investigated with the nose-boom installation.

INTRODUCTION

Pilot presentation of airspeed and altitude quantities is usually provided by pressure-type sensors. The primary error associated with pressure measurements on aircraft is generally position error, or error resulting from the disturbance at the pressure source caused by the interference of the aircraft on the flow field.

Two pressure-type airspeed-altitude systems have been used for pilot presentation in the X-15 flight research program. Static-pressure position-error calibration data have been obtained for both of these systems at subsonic and supersonic speeds.

The first system investigated was a nose-boom installation which provided both static-pressure and stagnation-pressure sensing. Limited data from this system are presented in references 1 and 2, which report the methods used in determining the maximum Mach number (3.31) and maximum altitude (136,500 ft) attained with the system. The second system investigated incorporates two manifolded fuselage flush static orifices and a pitot probe located ahead of the canopy.

Both systems were intended primarily as sources for pressure altitude and airspeed information for the pilot during landings; however, they have been used on a limited basis at higher speeds to supplement other available airspeed-altitude information to the pilot.

Calibration data have been obtained with the X-15 airplane at speeds greater than for any other manned aircraft. For application to the design of high-speed airspeed-altitude systems, this paper presents static-pressure calibration data for the two systems investigated to illustrate inherent position-error characteristics of these types of installations, especially at supersonic speeds. The methods used to obtain the static-pressure calibration differ from those used in previous Flight Research Center investigations (refs. 3 and 4) because of the high performance at which the X-15 data were obtained. Details of the methods are included in this paper. Inasmuch as the flush static source was not positioned for use at supersonic speeds, other possible locations for supersonic use are discussed with the aid of X-15 model wind-tunnel data. In addition, stagnation-pressure position error evidenced from the probe ahead of the canopy is presented for both subsonic and supersonic speeds.

SYMBOLS

C_p static-pressure coefficient, $\frac{\Delta p}{q}$

h_p pressure altitude above mean sea level, ft

Δh_p error in standard pressure altitude due to static-pressure error (true minus indicated)

M	free-stream Mach number
M'	indicated Mach number
ΔM	Mach number error ($M' - M$)
p	free-stream static pressure, lb/sq ft
p'	indicated static pressure, lb/sq ft
Δp	static-pressure error ($p' - p$), lb/sq ft
p_t	stagnation pressure, lb/sq ft
Δp_t	stagnation-pressure error (indicated minus true), lb/sq ft
q	dynamic pressure, lb/sq ft
q_c	true impact pressure ($p_t - p$), lb/sq ft
t	time, sec
x	longitudinal distance from tip of nose of airplane to survey location, in.
α	angle of attack, deg
β	angle of sideslip, deg
γ	ratio of specific heats for air
φ	meridian angle, measured from bottom fuselage centerline, deg

Subscripts:

b	measurement from ball nose
n	measurement from nose boom
p	measurement from pitot probe

AIRPLANE

The X-15 is a single-place, rocket-powered research airplane capable of speeds over 6,000 feet per second and altitudes greater than 300,000 feet. Carried under the wing of a modified B-52 aircraft, the X-15 is launched at an altitude of about 45,000 feet. Figures 1 and 2 are photographs of the airplane showing the nose boom and ball nose, respectively. Figure 3 is a three-view drawing of the X-15 with the ball-nose installation.

Airspeed-Altitude Instrumentation

Nose boom.- In early tests, the X-15 airplane was equipped with a standard NACA pitot-static tube. Figure 4 shows a bottom view of the detached tube. Dimensions of the tube, diameters, and arrangements of the static orifices are presented in reference 5. The static orifices used for recording purposes were located 63 inches forward of the tip of the aircraft nose. The stagnation-pressure head, which is relatively insensitive to angle of attack up to 32°, was the A-6 type discussed in reference 6.

Flush static system.- A flush static system, consisting of two manifolded orifices on the sides of the fuselage, 50 inches rearward of the leading edge of the ball nose and 2 inches above the centerline, was provided for pilot use on landings after the nose boom was replaced by the ball nose (described below). The orifices were located to provide minimum errors over the speed and angle-of-attack ranges experienced during landings.

Pitot probe.- Since the removal of the nose boom, the stagnation-pressure source of the pilot's subsonic airspeed-altitude system has been a pitot probe located directly ahead of the canopy, 70 inches rearward of the nose (fig. 5).

Ball nose.- The ball nose (fig. 6), which replaced the X-15 nose boom, is a spherical pressure-nulling type of airflow sensor (ref. 7) designed for operations at the high temperatures associated with aerodynamic heating and at low dynamic pressures. Of the five pressure orifices on the "ball," only the stagnation orifice was used for recording pressures.

Recording.- NACA aneroid absolute- and differential-pressure recorders were used to record static and differential pressures. Each pressure was recorded on both a high and low range cell of 0 to 30 inches and 0 to 3 inches of mercury. For some flights, sensitive differential cells (±0 to 3 inches of mercury) were used to measure the pressure difference between the ball nose and the pilot's pitot probe. For calculating Mach numbers, differential cells were used to measure impact pressures. For the ball-nose configuration, the cells were hooked up between the ball-nose stagnation-pressure port and the flush-static orifices.

METHODS AND PRECISION

Comparison of Calibration Methods

X-15 airspeed calibration data were obtained by use of radar and rawinsonde instruments. Radar data were provided by two of the three AFMTC-Mod II radars (modified SCR-584 radars) located on the X-15 High Range, one at the Flight Research Center and the other at Beatty, Nev. AN/GMD-1A rawinsonde measurements were obtained primarily by the Edwards rawinsonde station, operated by the U. S. Air Force Air Weather Service.

Radar errors.- Recent studies indicate that for typical X-15 high-performance flights radar velocities are determined to accuracies of 50 to 75 feet per second by comparing the data obtained simultaneously from the two Mod II radars. Similarly, altitude accuracies are within about 1,000 feet when optical boresight corrections are unavailable. For lower-performance and, hence, shorter-range flights for which optical boresight corrections are available, the altitude accuracies are within about 100 feet (ref. 3).

Rawinsonde errors.- Reference 8 specifies that the standard deviation error in radiosonde temperature measurements is near 1° C for altitudes up to approximately 50,000 feet; for above 50,000 feet, reference 9 states that the errors are within 1.5° C to 2.0° C. The accepted value in the standard deviation of the radiosonde pressure error is 3 millibars below 50,000 feet and somewhat less above 50,000 feet (ref. 8). Accuracy of rawinsonde wind-speed data is dependent on the attitude and elevation angle at which the data are recorded. According to reference 10, the accuracy of wind speed from the AN/GMD-1A set for an altitude of 50,000 feet is 1.8 knots, 7 knots, and 16 knots at elevation angles of 20°, 10°, and 6°, respectively.

Calibration methods.- Two methods are used in applying the radar and rawinsonde data to determine static-pressure error for calibrating the X-15 airspeed-altitude installations. The radar-phototheodolite method, referred to herein as the radar method, is described in references 3 and 11. This method correlates the altitude of the aircraft obtained by radar with ambient pressure ascertained from radiosonde measurements. The static pressures are then compared to the values of static pressures recorded in flight. Inasmuch as the nose-boom stagnation-pressure errors may be considered negligible for most flow conditions (see refs. 5, 6, 12, and 13), the ratio of stagnation or impact pressure to static pressure may be used to derive true Mach number.

The resolving power limit of the phototheodolite system was reached as a result of the expansion of the performance envelope. Therefore, most of the airspeed nose-boom calibration data, especially at the higher speeds, were obtained without boresight corrections.

The other method, referred to herein as the sonic method, determines Mach number by using the ratio of true velocity to the speed of sound based on ambient temperature from radiosonde measurements. Velocity, referenced to the ground, and altitude are obtained by radar. Winds and air temperature as functions of geometric altitude are obtained by rawinsonde measurements from which true velocity and speed of sound are determined in conjunction with radar measurements.

Comparison of calibration methods.- Figure 7 presents a comparison of approximate Mach number errors for various Mach numbers and pressure altitudes for both methods. For the radar method the following two errors were assumed: a 1,000-foot error in radar altitude, and a static-pressure error corresponding in part to a 1,000-foot radar error, and, in addition, to errors in the radiosonde pressure survey (an error that varies with altitude, estimated as ±250 feet at 50,000 feet and ±500 feet at 100,000 feet). For the sonic method, a constant velocity error of 50 feet per second and a constant temperature error of 2° C were assumed. Wind-velocity error is assumed to be negligible, since the

prevailing wind directions encountered during X-15 flights have been nearly normal to the flight path. For the error analysis, temperature and pressure values as a function of altitude were taken from reference 14.

Figure 7 shows that both methods are fairly insensitive to altitude and that the radar method is considerably more sensitive to Mach number than is the sonic method. The sonic method gives more accurate results than the radar method for Mach numbers slightly in excess of 2. Also, although not taken into account in figure 7, the radar method is increasingly affected by pressure lag as altitude increases, whereas the sonic method is not subject to lag, other than the insignificantly small amount incurred by the radiosonde temperature element in rising with the balloon.

Because the sonic method was more accurate than the radar method for Mach numbers greater than 2 when boresight corrections were no longer available, as a consequence of the increased tracking ranges, the sonic method was adopted exclusively for X-15 calibration purposes. As a result, all of the flush static data in this paper were determined by this method. As previously mentioned, the nose-boom calibration (obtained at shorter ranges) was achieved entirely by the radar method, although most of the data were determined without boresight corrections, especially at supersonic speeds. The small amount of data that contains boresight corrections is accurate to about 0.01 to 0.02 in Mach number, based on reference 4.

Interpretation of Recorded Static Pressures

Although the major pressure error is position error, the other errors must also be taken into account.

Recorder errors.- For both the nose-boom and flush static systems, NACA aneroid absolute-pressure and differential-pressure recorders were used. Each recorder had two cells with ranges of 0 to 30 inches and 0 to 3 inches of mercury. According to curves presented in reference 3, the maximum Mach number error resulting from static-pressure error associated with this combination of cells for altitudes up to 80,000 feet (the highest altitude at which calibration data were attained) is about 1 percent. However, for most altitudes for which the more-sensitive cell can be used (above about 50,000 ft) the errors are less than 0.25 percent. Similarly, from reference 3, it is estimated that the maximum error resulting from differential-pressure errors is 1 percent of the Mach number or less for the flight conditions of the calibration data.

Static-probe errors.- Wind-tunnel calibration data (see refs. 5, 12, and 13) indicate that the variation in static-pressure error of the standard NACA pitot-static tube caused by angle of attack is generally less than 1 percent of the impact pressure up to an angle of attack of 15°; the variations resulting from sideslip angles below 3° are less than 2 percent. These errors correspond to Mach number errors of 0.5 percent and 1 percent, respectively, at Mach numbers greater than 3 and 0.008 and 0.016 at a Mach number of 1. Nose-boom calibration data were not obtained, however, at sideslip angles greater than about 1°. Of course, the pressure errors for the flush static vents due to

small protuberances or variations in skin contour are not known, but they are not believed to be excessive (ref. 15).

Pressure lag.- Ground calibrations were made of the static-pressure lags of both systems. The sea-level-lag constant was determined to be 0.014 second for the nose-boom installation and 0.008 second for the flush static system. Calibration data for the nose-boom static pressures were corrected for lag when the resulting errors were in excess of 0.01 in Mach number. The calibration data for the flush static pressures were not corrected for lag. The errors are generally small, but errors near 0.04 in Mach number can result when data correspond to altitudes near 80,000 feet.

External flow effects.- The exhaust and intake of air out of and into the static orifices, caused by external interference, produce an effect similar to lag. From the results of investigations of this effect on the NACA type of pitot-static tube (refs. 16 and 17), it was determined that resulting Mach number errors are negligible for the X-15 installation. Therefore, no corrections were made for either system.

Specific-heat effects.- When the Rayleigh pitot formula (ref. 18) is used to calculate Mach number by the radar method, the variation of the ratio of specific heats for air γ must be considered at high stagnation temperatures for Mach numbers exceeding about 2. In the study of reference 1, values of γ were used from reference 19 for calculating the maximum Mach number achieved with the nose boom. Representative data from reference 1 are included in the calibration data presented in this paper. All of the remaining nose-boom calibration data presented were similarly corrected when the variation of γ caused an error in excess of 0.01 in Mach number. The maximum Mach number error was approximately 0.02, occurring at 3.31, the peak Mach number attained with the nose boom.

The flush static calibration data, obtained by the sonic method, are affected differently by γ than are the nose-boom data. Inasmuch as the radar and rawinsonde measurements are not significantly sensitive to γ variations, only the calculation of M' is materially affected by a varying specific-heat ratio. However, the M' data presented herein were not corrected for this variation. The calibration data presented, then, effectively show free-stream Mach number for values of γ based on the standard specific-heat ratio of 1.4. The difference between M and M', essentially, is the correction that should be applied to the pilot's Mach meter reading, since this meter is subject to the same position error and is calibrated by using the Rayleigh pitot formula based on a constant γ. A part of the scatter in M' based on $\gamma = 1.4$ is attributed to the different ambient temperatures encountered during calibration. It is estimated that the maximum scatter in M' due to this effect is only about 0.01. Reference 20 presents more detailed information on γ effects.

Summary.- The following table summarizes these errors, excluding nonambient effects for the flush static system:

Source	Nose boom		Flush static		
	M = 1	M = 3	M = 1	M = 3	M = 5
Recorder					
p	0.007	0.010	0.007	0.010	0.010
q_c	.008	0	.008	0	0
Static-probe errors					
α effects	.008	.015	-----	-----	-----
β effects	.008	.020	-----	-----	-----
Lag	0	.005	0	.02	.04
Flow effects	0	.002	0	Unknown	Unknown
γ effects	0	.01	0	.01	.01
Total	0.031	0.062	0.015+	0.040+	0.060+

The errors associated with lag, external flow effects, and γ effects are additive in a climb and tend to lower M'; whereas, the errors associated with γ are of the opposite sign to the other errors in a dive. It is assumed that signs of the recorder errors are not generally dependent on altitude changes.

RESULTS AND DISCUSSION

Pitot-Probe Pressure Measurements

Subsonic.- The accurate measurement of stagnation pressure on aircraft at subsonic speeds is usually attained easily with properly designed pitot probes (refs. 5, 6, and 21). With the nose-boom configuration, however, an undesirable sensitivity to angle of attack was evidenced in the stagnation-pressure measurements from the pilot's pitot probe ahead of the canopy (fig. 8(a)). The true stagnation pressures for the data of this figure were recorded from the nose boom.

The magnitudes of the errors shown in figure 8(a) were undesirable for airspeed presentation to the pilot for the very critical landing approaches of the X-15. A flight investigation was conducted, therefore, to find a more accurate probe or a better location for sensing stagnation pressure. A sleeve having a sharp lip and a 30° conical internal chamber to minimize flow-sensitivity effects (ref. 6) was attached to the pilot's pitot probe. An experimental probe with basic geometry similar to the modified probe was installed at station 17, on the top of the fuselage at the centerline. Figures 8(b) and 8(c) show that no improvement resulted from pressures measured by these two probes.

When the nose boom was replaced with the ball nose, the investigation using a calibrated reference stagnation source was necessarily terminated. By comparing the stagnation pressures recorded from the pilots' pitot probe with those recorded from the ball nose, it was found that the pressures sensed by the pilots' pitot probe were not affected by angle of attack for the ball-nose configuration at subsonic speeds. Figure 9, which shows the ratio of stagnation pressure measured by the pitot probe to that measured by the ball nose as a function of Mach number for 5° increments of angle of attack, indicates that no significant differences occur at subsonic speeds.

An X-15 model wind-tunnel investigation (ref. 22) both verifies and explains the results of the flight data. This investigation showed that stagnation pressures measured in the proximity of the X-15 pilots' probe are sensitive to angle of attack when the nose of the aircraft includes a nose boom. But, for either a rounded or pointed nose, the stagnation pressures were found to be insensitive to angle of attack. Reference 22 concludes that the stagnation-pressure errors probably result from the vorticity shed by the nose boom.

Supersonic.- Figure 9 shows that stagnation-pressure calibration data obtained at supersonic speeds are considerably affected by angle of attack above $M = 1.8$, due to local flow characteristics, complicated by the location of the probe behind the aircraft bow wave. The data can be approximated by calculated curves as shown for angles of attack of 0°, 10°, and 20° (assuming no errors in stagnation pressures sensed by the ball nose). The curves for 0° and 10° were calculated by using the well-known tangent-cone approximation; the curve for 20° was calculated by using a Prandtl-Meyer expansion from the tip of the nose back to the probe station. The curves, in general, agree with the data, even though secondary factors such as vortex effects were not included.

In contrast to stagnation pressures sensed by the pilots' pitot probe, the stagnation pressures sensed by the ball nose are not subject to angle-of-attack effects, inasmuch as the ball is affected only by a normal shock. The stagnation-pressure losses behind the normal shock can be accurately determined by the Rayleigh pitot formula, except for extreme rarefied flow conditions (see refs. 23 and 24).

Static-Pressure Position-Error Calibrations

Subsonic and transonic.- Figures 10 and 11 show the subsonic and transonic calibration data in terms of free-stream Mach number and indicated Mach number for the nose-boom installation and the flush static installation, respectively. The nose-boom calibration data are not referenced to angle of attack, since these data, as well as other NACA standard nose-boom flight data, have shown the angle-of-attack effects to be small up to $\alpha \approx 12°$. The position error characteristically drops to near zero at a Mach number slightly greater than 1.0, corresponding to the passage of the aircraft bow wave.

The flush static calibration data (fig. 11) are shown for various angles of attack. Sensitivity of position error to angle of attack for subsonic speeds is not evident from the data.

Supersonic.- The calibrations for the two systems for Mach numbers greater than 1.2 are presented in figure 12 and in figures 13(a) and 13(b). Again, as for subsonic speeds, no effect of angle of attack was expected, or found, for the nose-boom calibration. However, for Mach numbers greater than 2, the data indicate that the position error increases significantly with Mach number. Apparently, these errors are caused by the interference of the NACA pitot-static tube with the flow field, rather than the interference of the airplane with the field, inasmuch as the airplane bow wave is well to the rear of the static orifices. Included in the figure are data, for $\alpha = 0°$, of an isolated pitot-static tube calibrated in a wind tunnel, as reported in reference 15.

The flush static calibration (figs. 13(a) and (b)) at supersonic speeds shows much larger errors than the nose-boom calibration (fig. 12). Large variations with angle of attack are evidenced, despite scatter. The higher angle-of-attack data reflect smaller position errors.

Flush static sideslip effects.- The flush static system incorporates two manifolded orifices, as previously described, for reducing the static-pressure errors caused by sideslip. No position-error effect has been found for sustained angle of sideslip up to about 3°. However, for oscillatory angle-of-sideslip changes, definite sensitivity has been exhibited, as seen in figure 14 which shows M', M, and β during different periods of a flight. Although these errors are not generated in stable flight and do not materially affect the pilots' performance, they do indicate that diametrically opposed side-fuselage orifices even when manifolded do not always compensate for variations in sideslip.

Comparison of Position-Error Calibrations

Figures 15(a) and 15(b) compare the position-error calibrations of the two systems in terms of M, Δh_p, and $\frac{\Delta p}{q_c}$. The curves were determined from the calibration data presented in the preceding section. The curves for the NACA pitot-static tube were used for correcting Mach number and pressure altitude in reducing basic X-15 flight data. The curves for the flush static system, shown up to a maximum Mach number of 4 for three angles of attack, are not accurate calibration curves for reduction of basic flight data above $M \approx 1$, but are included to provide a general comparison with the nose-boom data.

Subsonically, the two systems result in Mach number and pressure-altitude errors of approximately the same magnitudes. Supersonically, the systems indicate markedly different magnitudes of errors. The maximum Mach number and pressure-altitude errors for the nose-boom installation are 0.18 and 2,200 feet, respectively, occurring at the maximum Mach number of 3.31 attained with the nose-boom installation. At the same Mach number, the corresponding errors for the flush static system are 0.88 and 12,400 feet for $\alpha = 0°$ and 0.50 and 6,300 feet for $\alpha = 12°$. For the flush static system, as with the nose-boom installation, the maximum Mach number and altitude errors occur at the maximum Mach number tested. These errors are 1.25 in Mach number and 15,200 feet in

altitude for $\alpha = 0°$ and 0.77 and 8,800 feet for $\alpha = 12°$ at a Mach number of 4.

Unlike the errors associated with the flush static system, which are attributed to aircraft disturbance of the ambient-pressure field, the errors for the nose-boom installation can be almost entirely attributed to tube disturbance of the airflow at supersonic speeds. Once a particular pitot-static tube is calibrated in a wind tunnel, it may be installed on any nose boom of nominal length without an extensive flight calibration at supersonic speeds, with one minor exception: It is sometimes necessary to calibrate for the effect of the aircraft bow-wave interaction with the boundary layer which may cause a complex shock pattern in the vicinity of the pitot-static-tube orifices. This error is small, however, and is limited to a narrow Mach number range at low supersonic speeds (ref. 25).

Analysis of Possible Static-Pressure-Sensing Locations

Nose section.- The data of figures 13(a) and 13(b) illustrate the importance of selecting fuselage static orifices that result in minimum pressure sensitivity to angle of attack at supersonic speeds. Another consideration in the selection of fuselage orifices for supersonic use is to minimize associated static-pressure coefficients C_p which are approximately constant with Mach number at a constant angle of attack. This is important because as dynamic pressure increases with the square of Mach number, the static-pressure error increases at the same rate to keep the coefficient constant. Figure 16 shows the Mach number errors that correspond to various values of static-pressure coefficient over the Mach number range from 0 to 10.

With the preceding considerations as prime requisites, X-15 model wind-tunnel static-pressure data (refs. 26 and 27) were analyzed to find an optimum location on the X-15 ogive nose for sensing static pressures at supersonic speeds. Figure 17 shows the variations of static-pressure coefficient for fuselage station 50 against fuselage circumferential angle for various Mach numbers and angles of attack. Apparently, a meridian angle between 80° and 85° would be better than the now-used 98° for decreasing static-pressure sensitivity to angle of attack for the supersonic Mach numbers investigated. However, the average static-pressure coefficient of 0.1 would be about the same as experienced at the present location.

Figure 18 is presented to show the mean magnitude of static-pressure coefficient corresponding to the meridian angle that results in minimum sensitivity to angle of attack for various stations on the nose. Apparently, only circumferential locations (specified in following figure) near station 131 would result in both minimum pressure sensitivity to angle of attack and mean values of the static-pressure coefficient near zero. A closer inspection of the wind-tunnel data for fuselage station 131 (fig. 19) indicates that a meridian angle of approximately 80° appears to be optimum for the Mach number range from 2.30 to 4.65. However, a variation of about ±0.025 in static-pressure coefficient would occur for angle-of-attack variations from 0° to 15°, which is similar to the static-pressure-coefficient variation with angle of attack for the best circumferential location at station 50 (fig. 17).

Analysis of the wind-tunnel data shows that no location on the fuselage nose of the X-15 is significantly insensitive to angle-of-attack variations for Mach numbers between 2.30 and 4.65.

Base locations.- Base pressure measurements on the X-15 (ref. 28) indicate that static-pressure coefficients may be less affected by angle of attack at base locations than at locations on the ogive nose. However, additional research is needed to ascertain if significant improvement could be gained by utilizing base pressures for airspeed applications.

CONCLUSIONS

Static-pressure and stagnation-pressure calibration data obtained to define position errors both subsonically and supersonically for the various airspeed-altitude installations on the X-15 airplane led to the following conclusions:

1. Stagnation pressures from the pilots' pitot probe located ahead of the canopy were very sensitive to angle of attack above a Mach number of 1.8, since the probe was not located ahead of the aircraft bow wave.

2. The nose-boom static pressures, although relatively insensitive to angle of attack up to the maximum encountered of 12°, resulted in Mach number and pressure-altitude errors that increased with Mach number. At the maximum Mach number of 3.31 attained with the nose boom, the absolute errors were 0.18 in Mach number and 2,200 feet in pressure altitude.

3. The flush static system, unlike the nose-boom system, was significantly sensitive to angle of attack at supersonic speeds. At a Mach number of 3.31, the absolute Mach number and pressure-altitude errors were 0.88 and 12,400 feet, respectively, for 0° angle of attack; for the same Mach number, but at an angle of attack of 12°, the corresponding absolute Mach number and pressure-altitude errors were 0.50 and 6,300 feet, respectively.

4. Similar to the nose-boom installation, above the transonic region the Mach number and pressure-altitude errors of the flush static system increased with Mach number. The errors at a Mach number of 4.0 for an angle of attack of 0° resulted in Mach number and pressure-altitude errors of 1.25 and 15,200 feet, respectively.

5. The study indicated that a nose-boom static-pressure installation is more suitable from the standpoint of position error and ease of calibration than a flush static system in the speed range from low subsonic to the highest Mach number (3.31) investigated with the nose-boom installation.

Flight Research Center
National Aeronautics and Space Administration
Edwards, Calif., December 7, 1962

REFERENCES

1. Stillwell, Wendell H., and Larson, Terry J.: Measurement of the Maximum Speed Attained by the X-15 Airplane Powered With Interim Rocket Engines. NASA TN D-615, 1960.

2. Stillwell, Wendell H., and Larson, Terry J.: Measurement of the Maximum Altitude Attained by the X-15 Airplane Powered With Interim Rocket Engines. NASA TN D-623, 1960.

3. Brunn, Cyril D., and Stillwell, Wendell H.: Mach Number Measurements and Calibrations During Flight at High Speeds and at High Altitudes Including Data for the D-558-II Research Airplane. NACA RM H55J18, 1956.

4. Larson, Terry J., Stillwell, Wendell H., and Armistead, Katharine H.: Static-Pressure Error Calibrations for Nose-Boom Airspeed Installations of 17 Airplanes. NACA RM H57A02, 1957.

5. Pearson, Albin O., and Brown, Harold A.: Calibration of a Combined Pitot-Static Tube and Vane-Type Flow Angularity Indicator at Transonic Speeds and at Large Angles of Attack or Yaw. NACA RM L52F24, 1952.

6. Gracey, William: Wind-Tunnel Investigation of a Number of Total-Pressure Tubes at High Angles of Attack. Subsonic, Transonic, and Supersonic Speeds. NACA Rep. 1303, 1957. (Supersedes NACA TN 3641.)

7. Anon.: Technical Description and Operating Instructions — N.A.S.A. Flow-Direction and Pitot-Pressure Sensor. NORT 60-46, Nortronics, Div. of Northrop Corp., 1960.

8. Anon.: Accuracies of Radiosonde Data. AWS Tech. Rep. 105-133, Military Air Transport Service, U. S. Air Force, Sept. 1955.

9. Anon.: Temperatures at the 10-mb (101,000-Foot) Level. AWS Tech. Rep. 105-108, Military Air Transport Service, U. S. Air Force, May 1953.

10. Campen, C. F., Jr., Cole, A. E., Condron, T. P., Ripley, W. S., Sissenwine, Norman, and Solomon, Irving, eds.: Handbook of Geophysics for Air Force Designers. First ed., Geophysics Res. Directorate, Air Force Cambridge Res. Center, 1957.

11. Zalovcik, John A.: A Radar Method of Calibrating Airspeed Installations on Airplanes in Maneuvers at High Altitudes and at Transonic and Supersonic Speeds. NACA Rep. 985, 1950.

12. Sinclair, Archibald R., and Mace, William D.: Wind-Tunnel Calibration of a Combined Pitot-Static Tube and Vane-Type Flow-Angularity Indicator at Mach Numbers of 1.6 and 2.01. NACA TN 3808, 1956.

13. Richardson, Norman R., and Pearson, Albin O.: Wind-Tunnel Calibrations of a Combined Pitot-Static Tube, Vane-Type Flow-Direction Transmitter, and Stagnation-Temperature Element at Mach Numbers From 0.60 to 2.87. NASA TN D-122, 1959.

14. Minzner, R. A., Champion, K. S. W., and Pond, H. L.: The ARDC Model Atmosphere, 1959. Air Force Surveys in Geophysics No. 115 (AFCRC-TR-59-267), Air Force Cambridge Res. Center (Bedford, Mass.), Aug. 1959.

15. Sommerville, T. V., and Jefferies, R. L.: Note on Model Tests of Static Vents. Effect of Degrees of Flushness, Waviness of Skin and Proximity of Rivets. B. A. Dept. Note — Wind Tunnels No. 531, British R. A. E., Sept. 1941.

16. Silsby, Norman S.: External Interference Effects of Flow Through Static-Pressure Orifices of an NACA Airspeed Head at a Mach Number of 3. NACA TN 4122, 1957.

17. Silsby, Norman S.: External Interference Effects of Flow Through Static-Pressure Orifices of an Airspeed Head at Several Supersonic Mach Numbers and Angles of Attack. NASA Memo 2-13-59L, 1959.

18. Dommasch, Daniel O., Sherby, Sydney S., and Connolly, Thomas F.: Airplane Aerodynamics. Second ed., Pitman Publishing Co., 1957.

19. Hansen, C. Frederick: Approximations for the Thermodynamic and Transport Properties of High-Temperature Air. NASA TR R-50, 1959.

20. Hill, Jacques A. F., Baron, Judson R., and Schindel, Leon H.: Mach Number Measurements in High-Speed Wind Tunnels. Tech. Rep. 145, Mass. Inst. Technology, Naval Supersonic Lab., Jan. 1956. (AFOSR Tech. Rep. 56-7, AD-81540.)

21. Huston, Wilber B.: Accuracy of Airspeed Measurements and Flight Procedures. NACA Rep. 919, 1948.

22. Alford, William J., Jr.: Subsonic Wind-Tunnel Investigation of Errors Indicated by Total-Pressure Tubes in the Flow Field of a Body Simulating the Nose of the X-15 Research Airplane. NASA TN D-1250, 1962.

23. Sherman, F. S.: New Experiments on Impact-Pressure Interpretation in Supersonic and Subsonic Rarefied Air Streams. NACA TN 2995, 1953.

24. Kane, E. D., and Maslach, G. J.: Impact-Pressure Interpretation in a Rarefied Gas at Supersonic Speeds. NACA TN 2210, 1950.

25. Gracey, William: Measurement of Static Pressure on Aircraft. NACA Rep. 1364, 1958. (Supersedes NASA TN 4184.)

26. Osborne, Robert S., and Stafford, Virginia C.: Basic Pressure Measurements on a 0.0667-Scale Model of the North American X-15 Research Airplane at Transonic Speeds. NASA TM X-344, 1960.

27. Hodge, B. Leon, and Burbank, Paige B.: Pressure Distribution of a 0.0667-Scale Model of the X-15 Airplane for an Angle-of-Attack Range of 0° to 28° at Mach Numbers of 2.30, 2.88, and 4.65. NASA TM X-275, 1960.

28. Saltzman, Edwin J.: Preliminary Base Pressures Obtained From the X-15 Airplane at Mach Numbers From 1.1 to 3.2. NASA TN D-1056, 1961.

Figure 1.- Photograph of the X-15 airplane with nose boom. E-5250

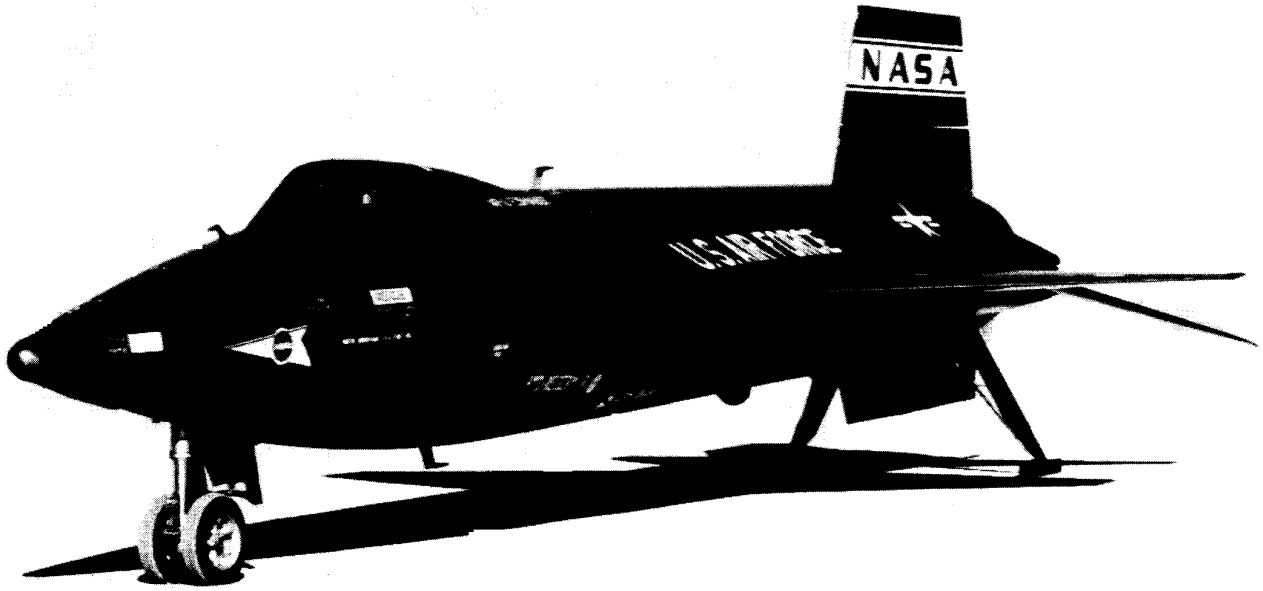

Figure 2.- Photograph of the X-15 airplane with ball nose. E-7902

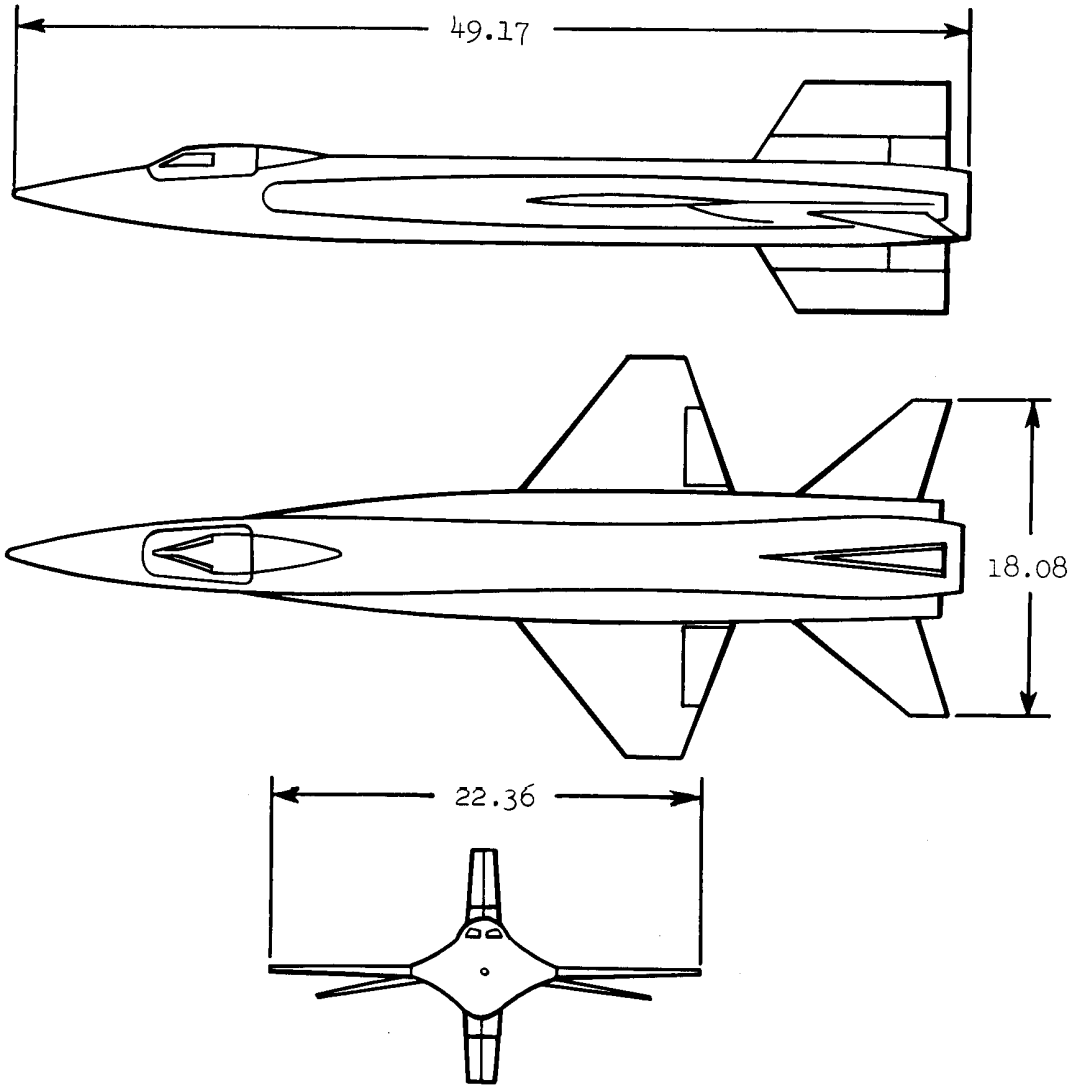

Figure 3.- Three-view drawing of the X-15 with ball nose. All dimensions in feet.

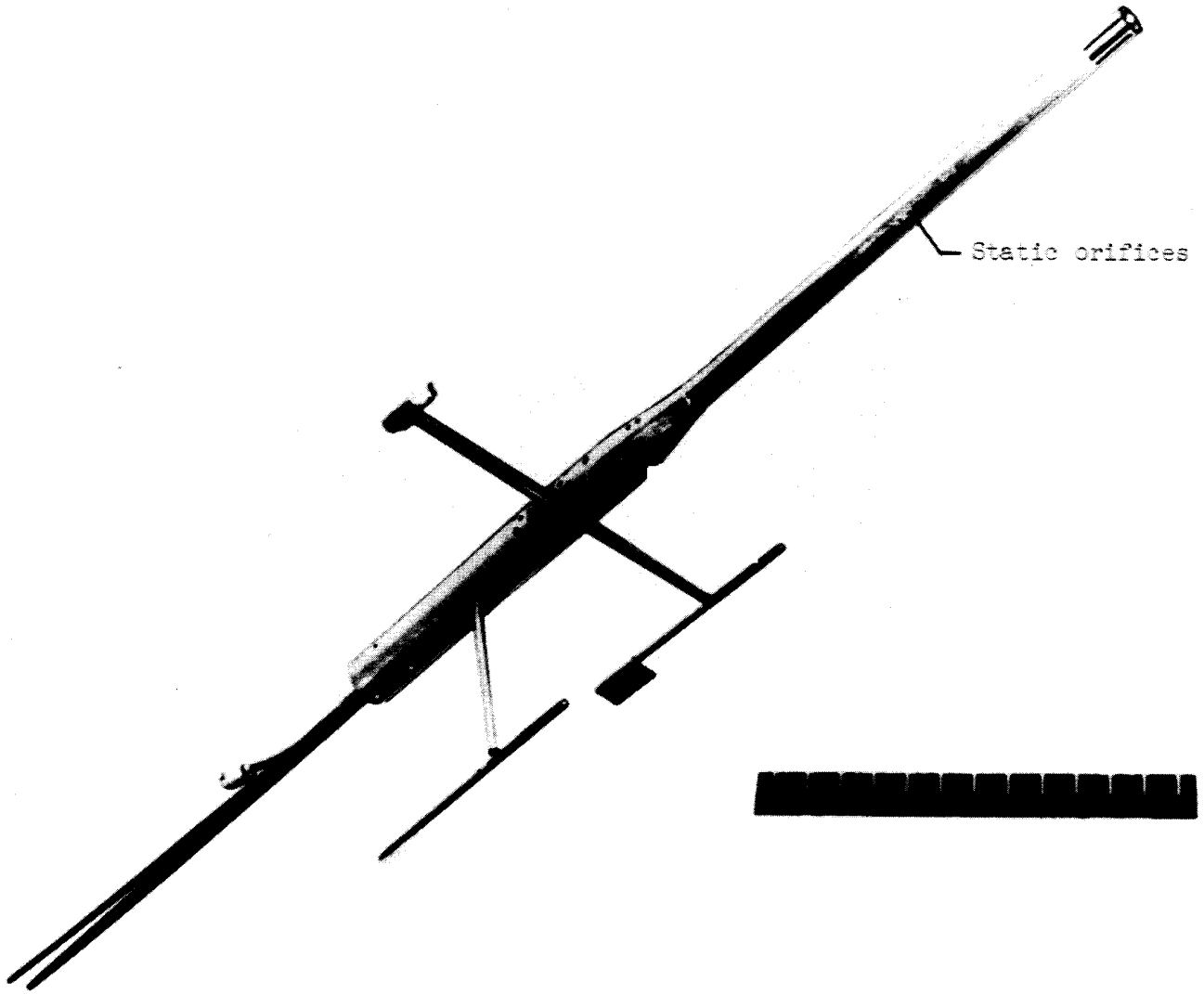

Figure 4.- Bottom view of X-15 nose-boom pitot-static tube.

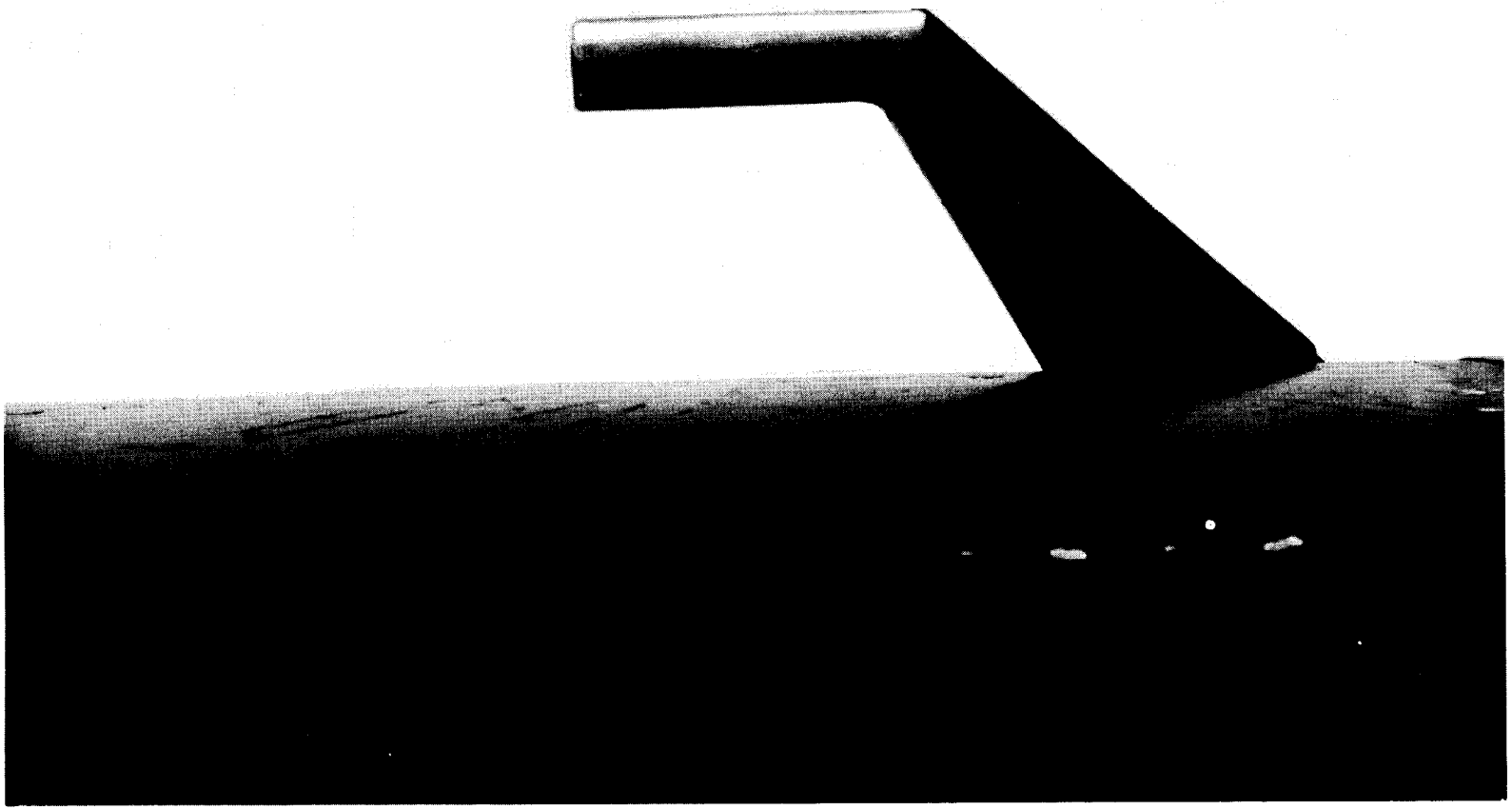

Figure 5.- Photograph of pilot's pitot probe.

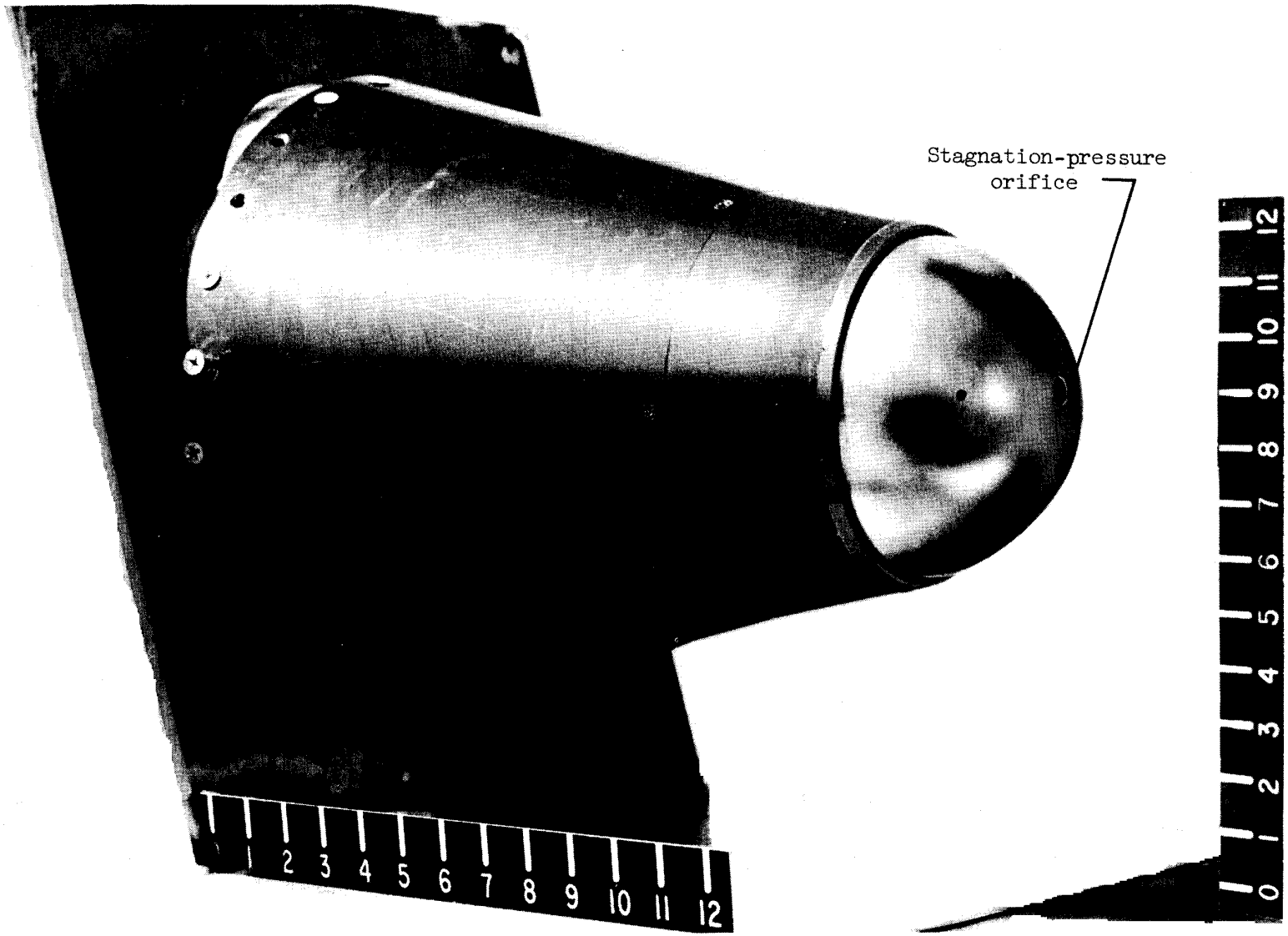

Figure 6.- Photograph of X-15 ball nose.

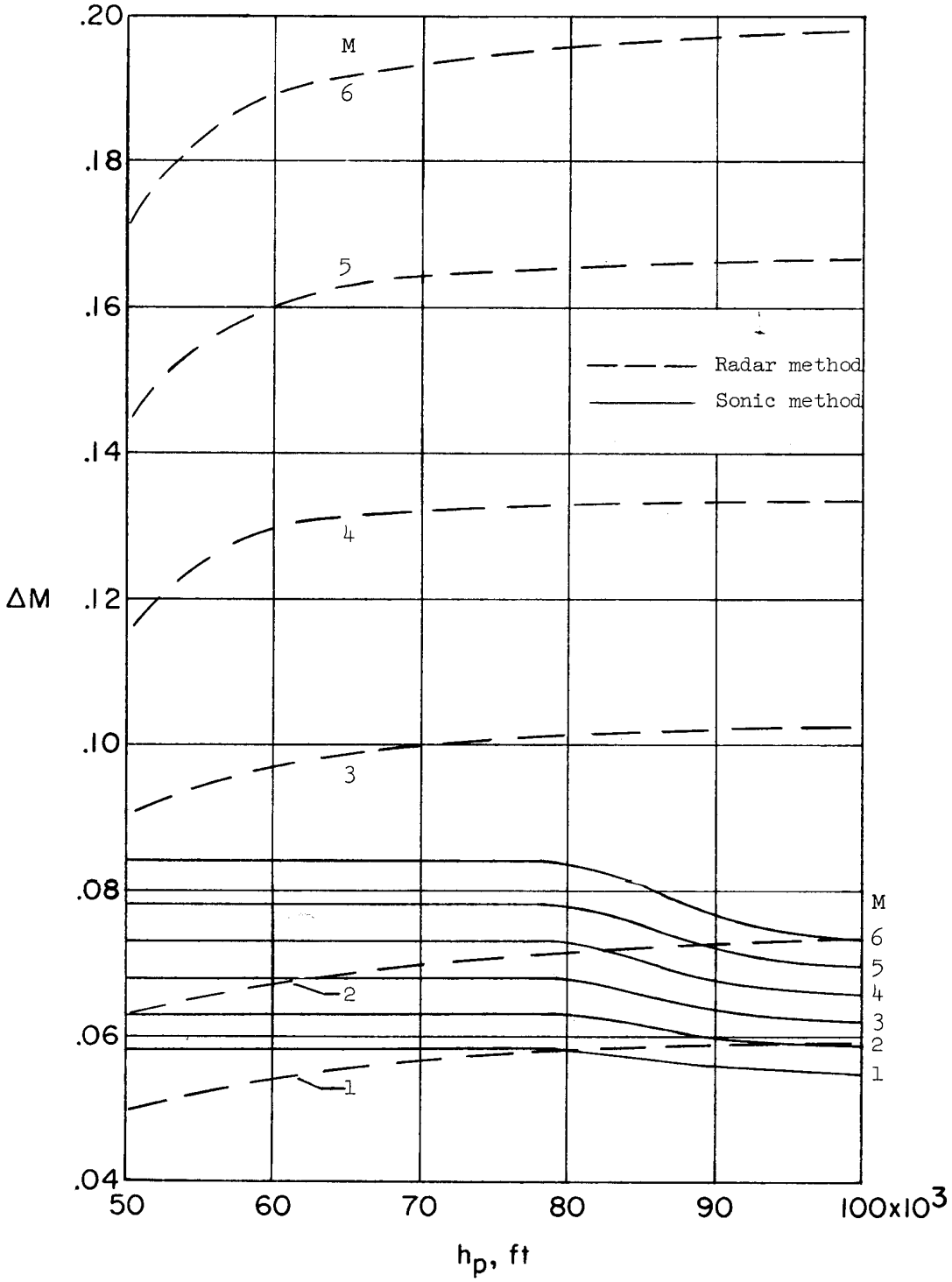

Figure 7.- Comparison of accuracies of calibration methods.

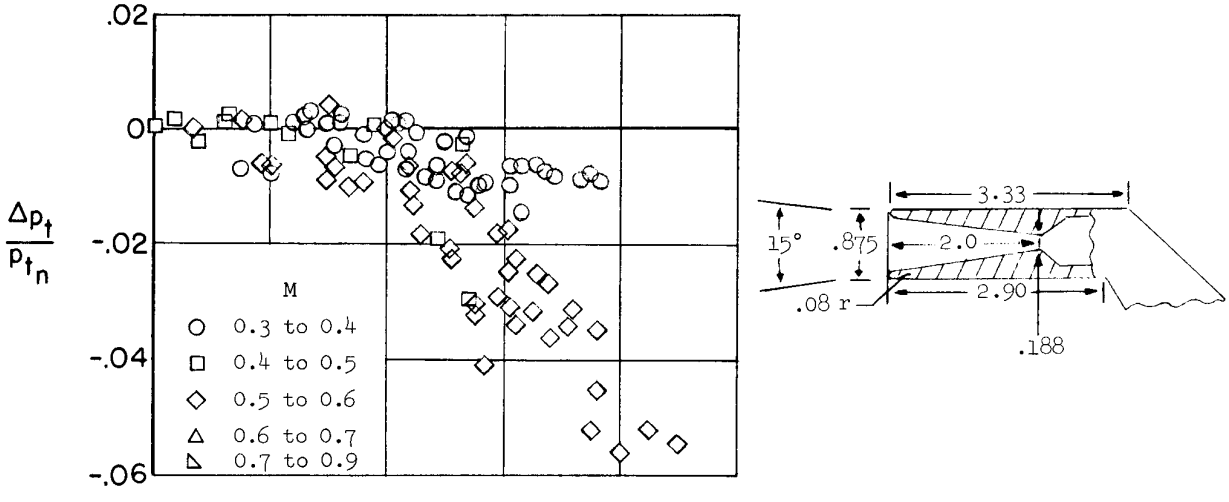

(a) Basic probe; station 68.

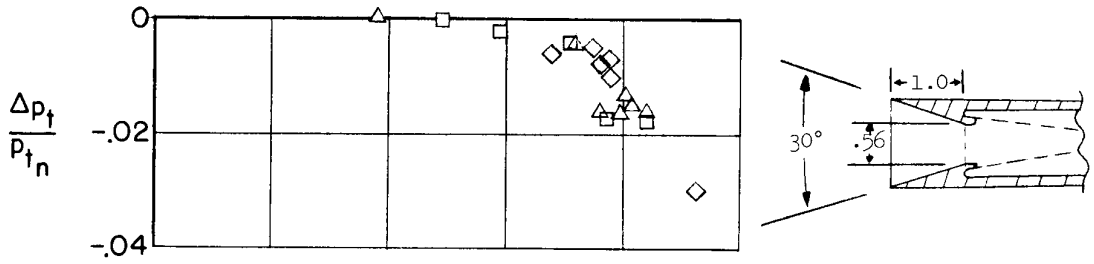

(b) Modified probe; station 68.

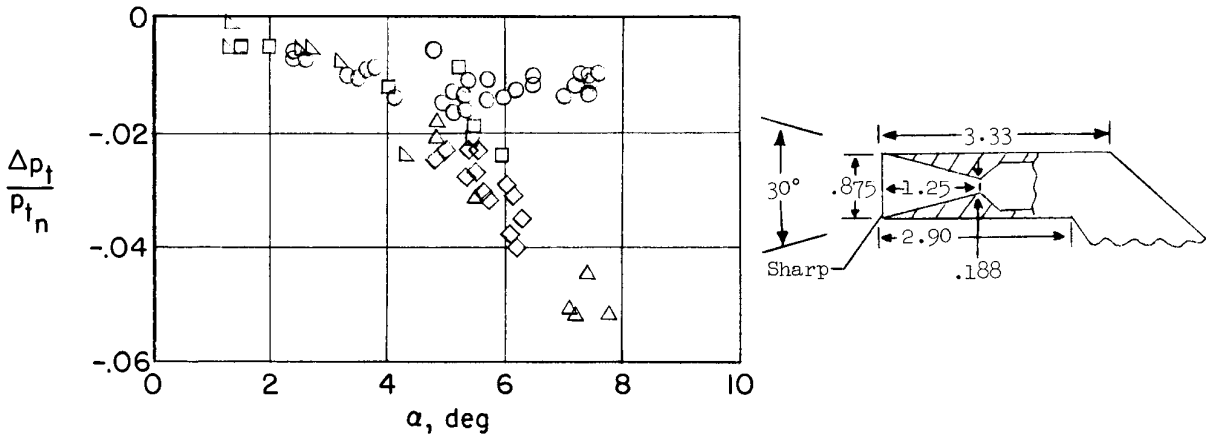

(c) New probe; station 17 (top centerline).

Figure 8.- Variation of subsonic total-pressure errors with angle of attack for three probes. Nose-boom configuration.

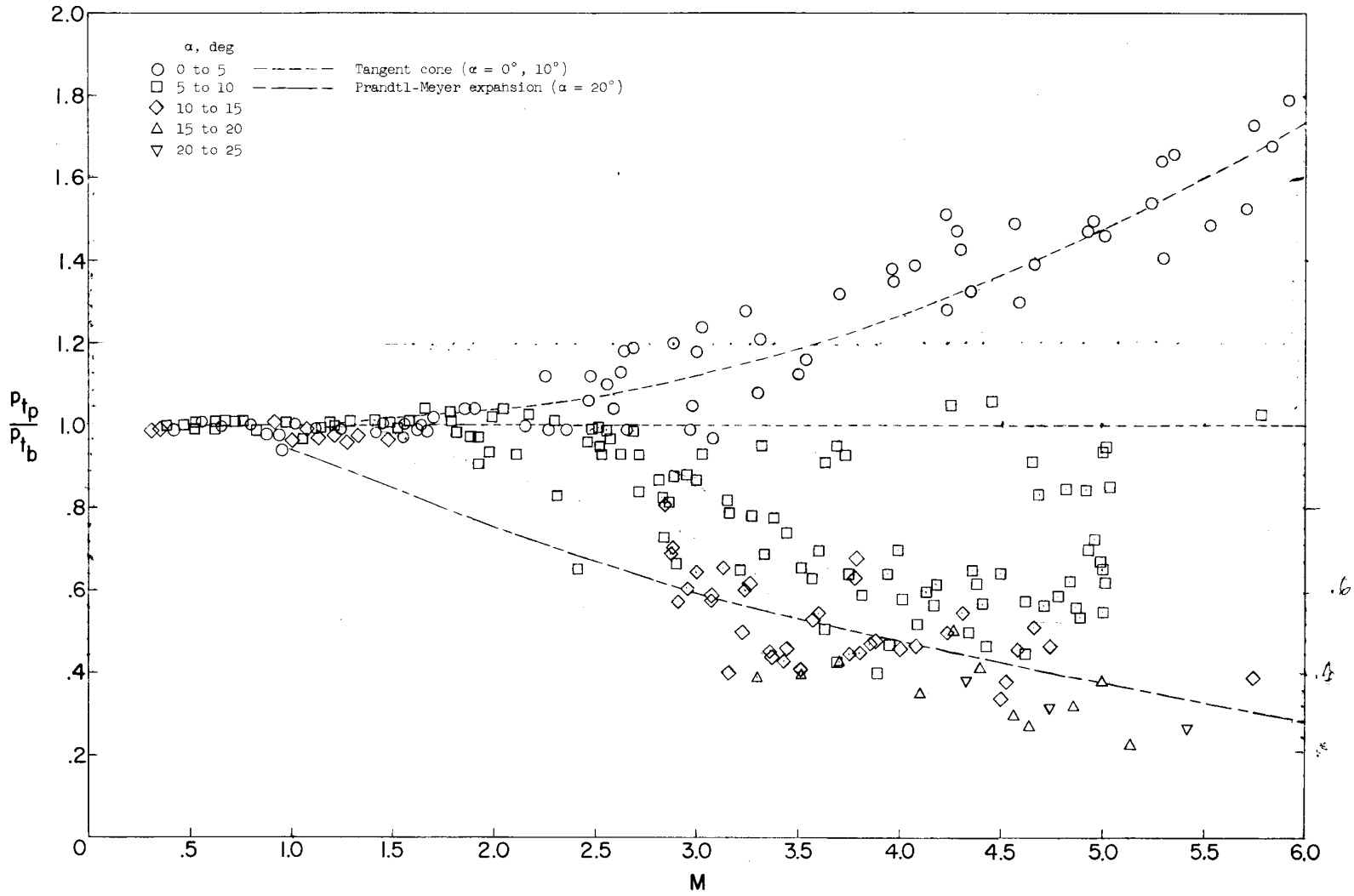

Figure 9.- Ratio of stagnation pressure measured by pilot's pitot probe to the stagnation pressure measured by the ball nose as a function of Mach number.

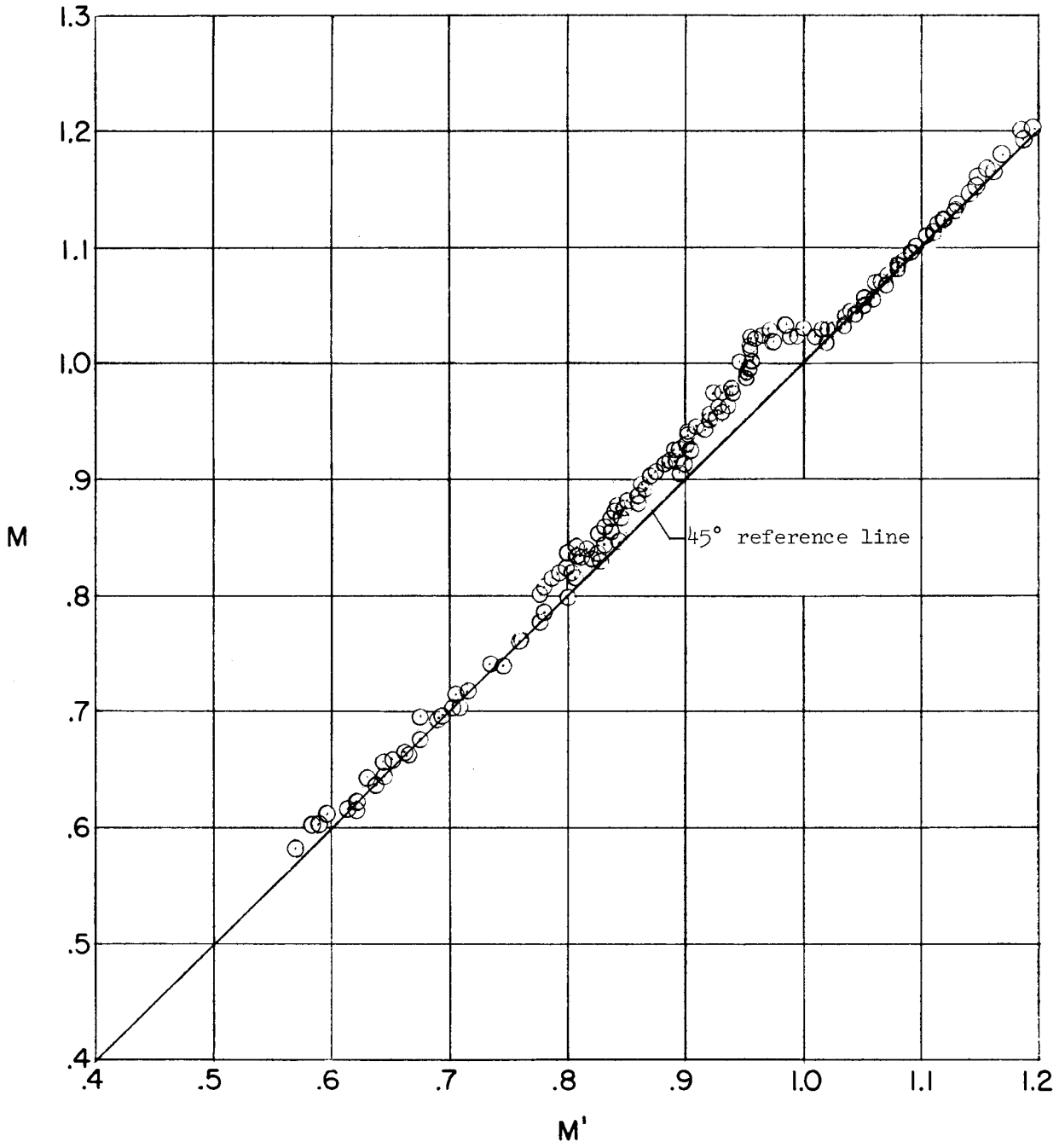

Figure 10.- Subsonic and transonic position-error calibration for the nose-boom system. α = 0° to 12°.

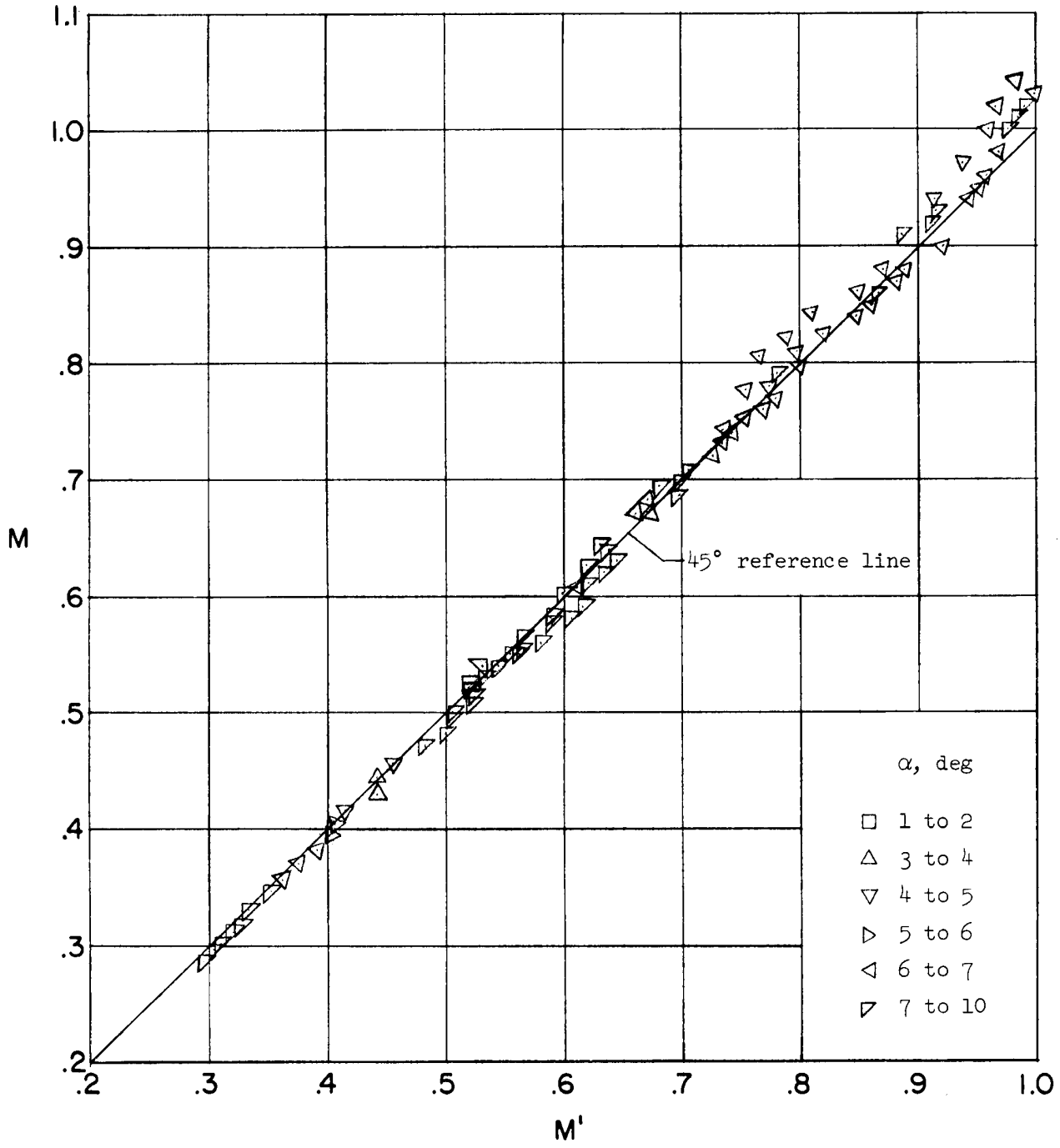

Figure 11.- Subsonic and transonic position-error calibration for the flush static (ball nose) system.

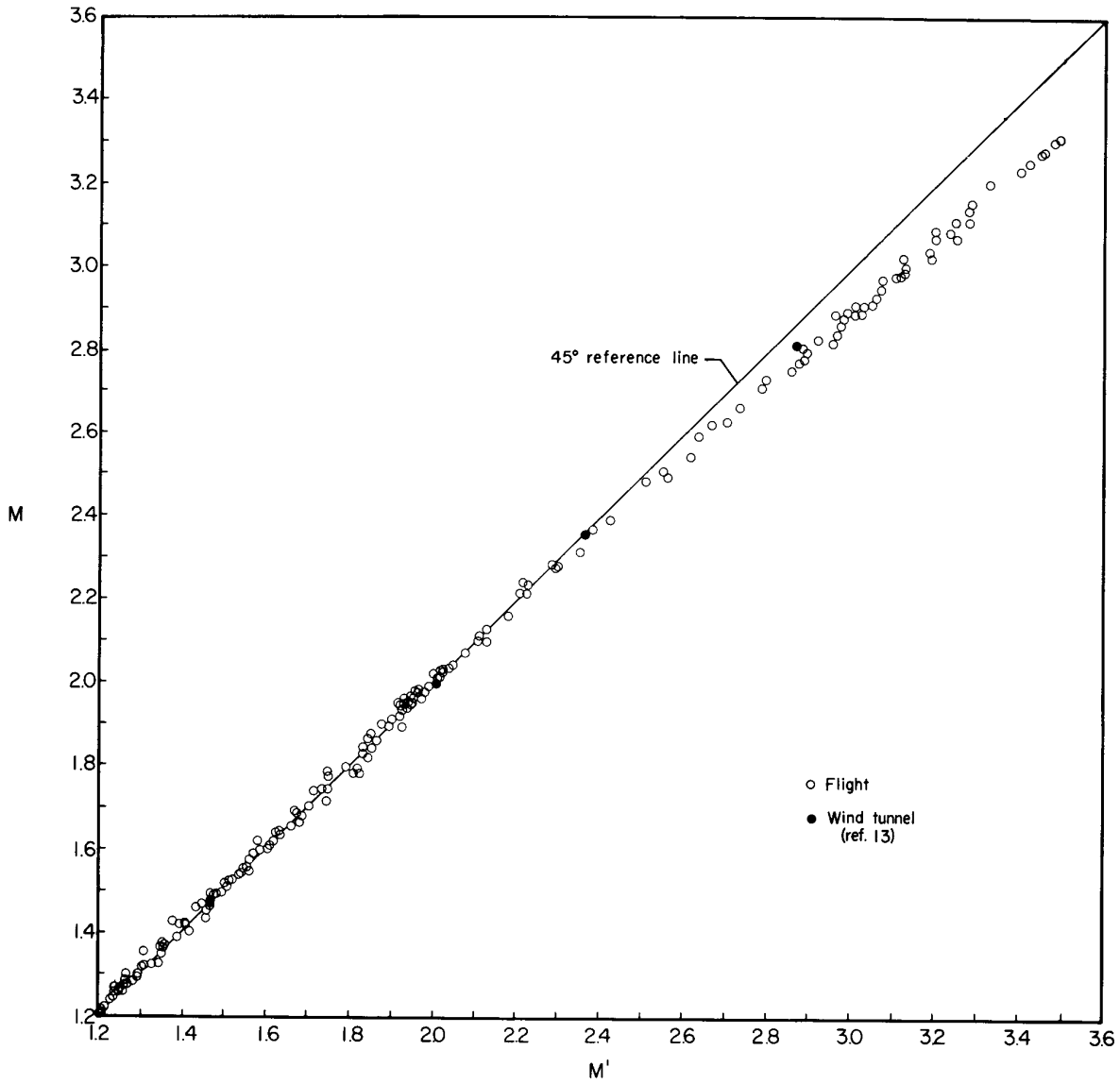

Figure 12.- Supersonic position-error calibration for the nose-boom system.

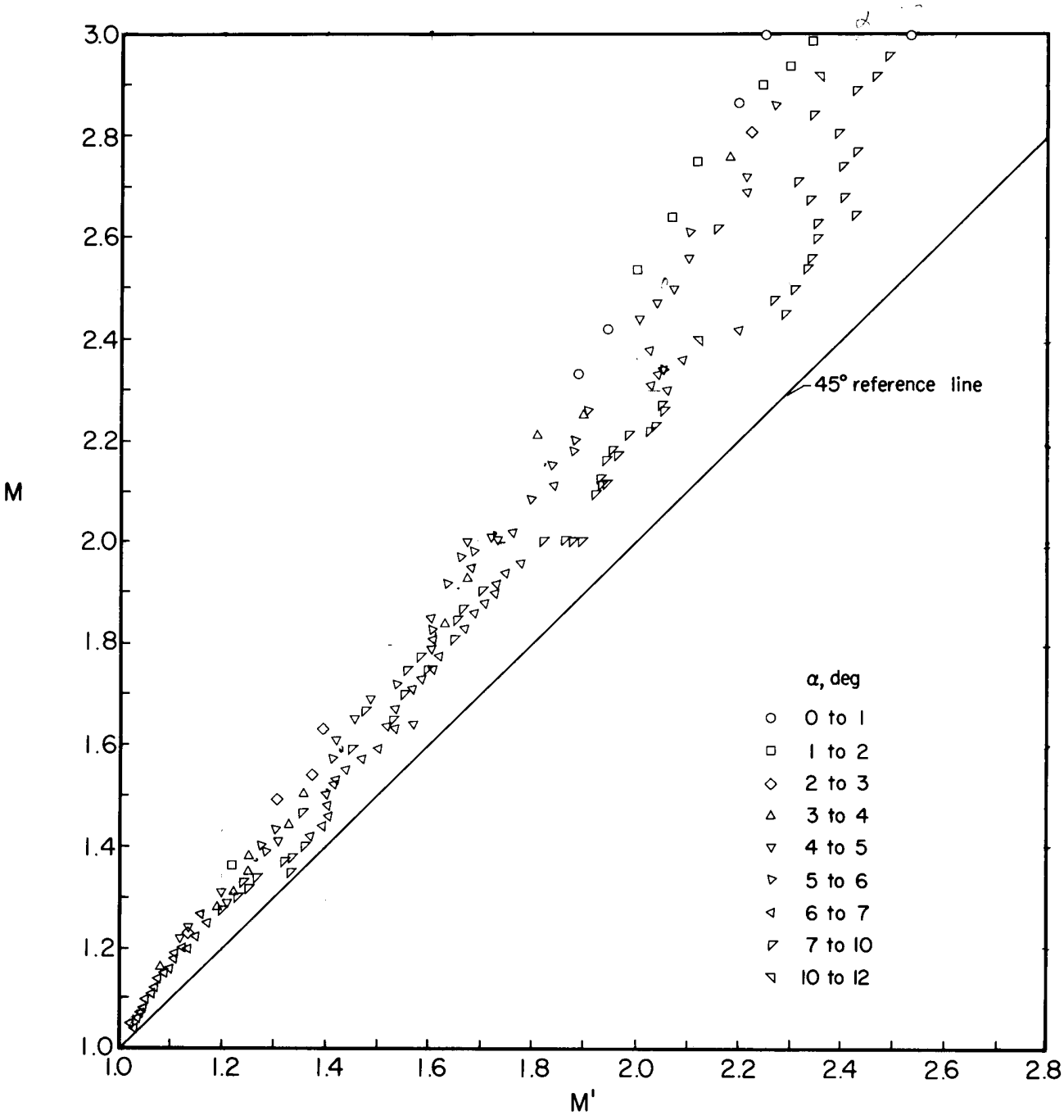

(a) M = 1.0 to 3.2.

Figure 13.- Supersonic position-error calibration for the flush static (ball nose) system.

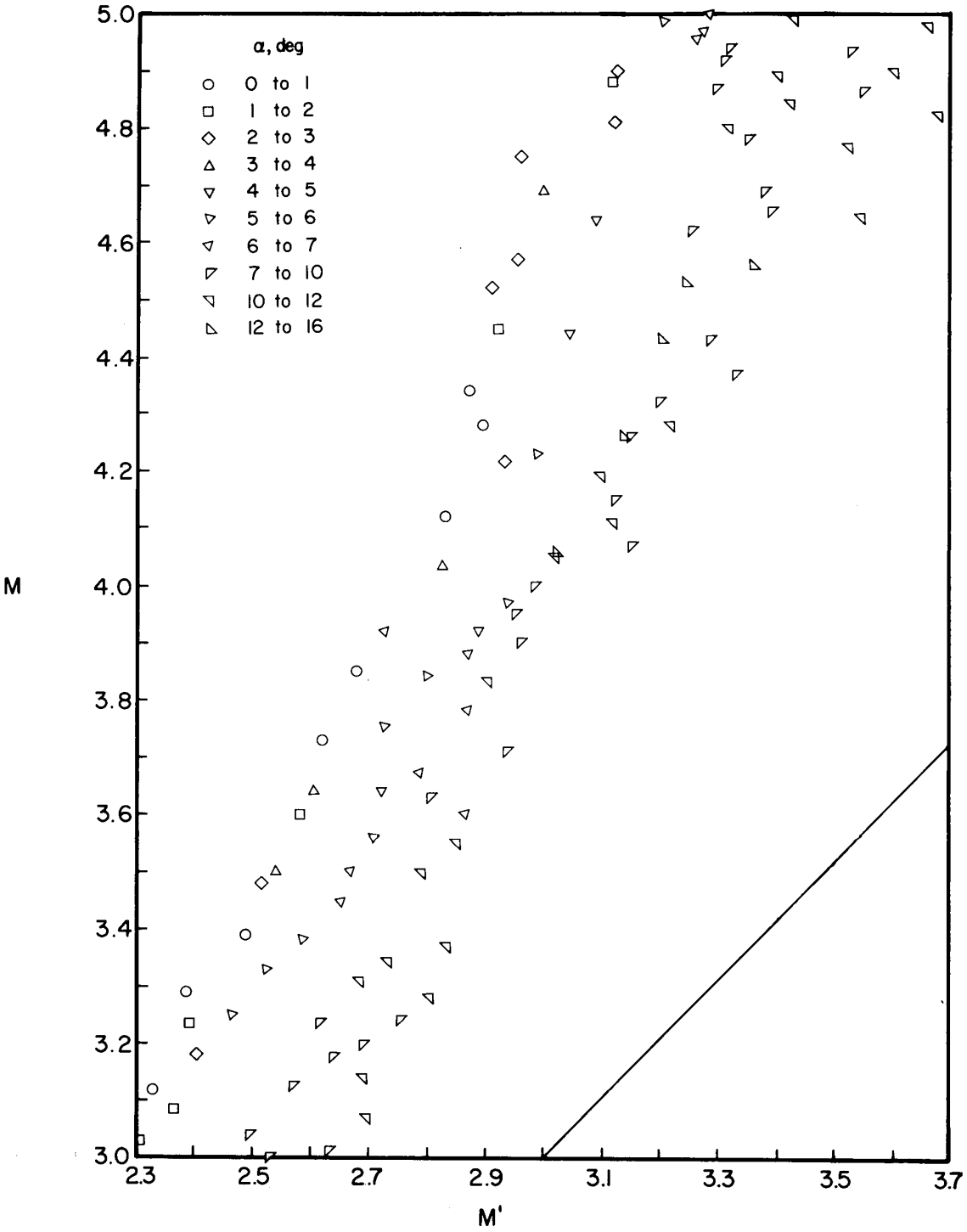

(b) M = 3.0 to 5.0.

Figure 13.- Concluded.

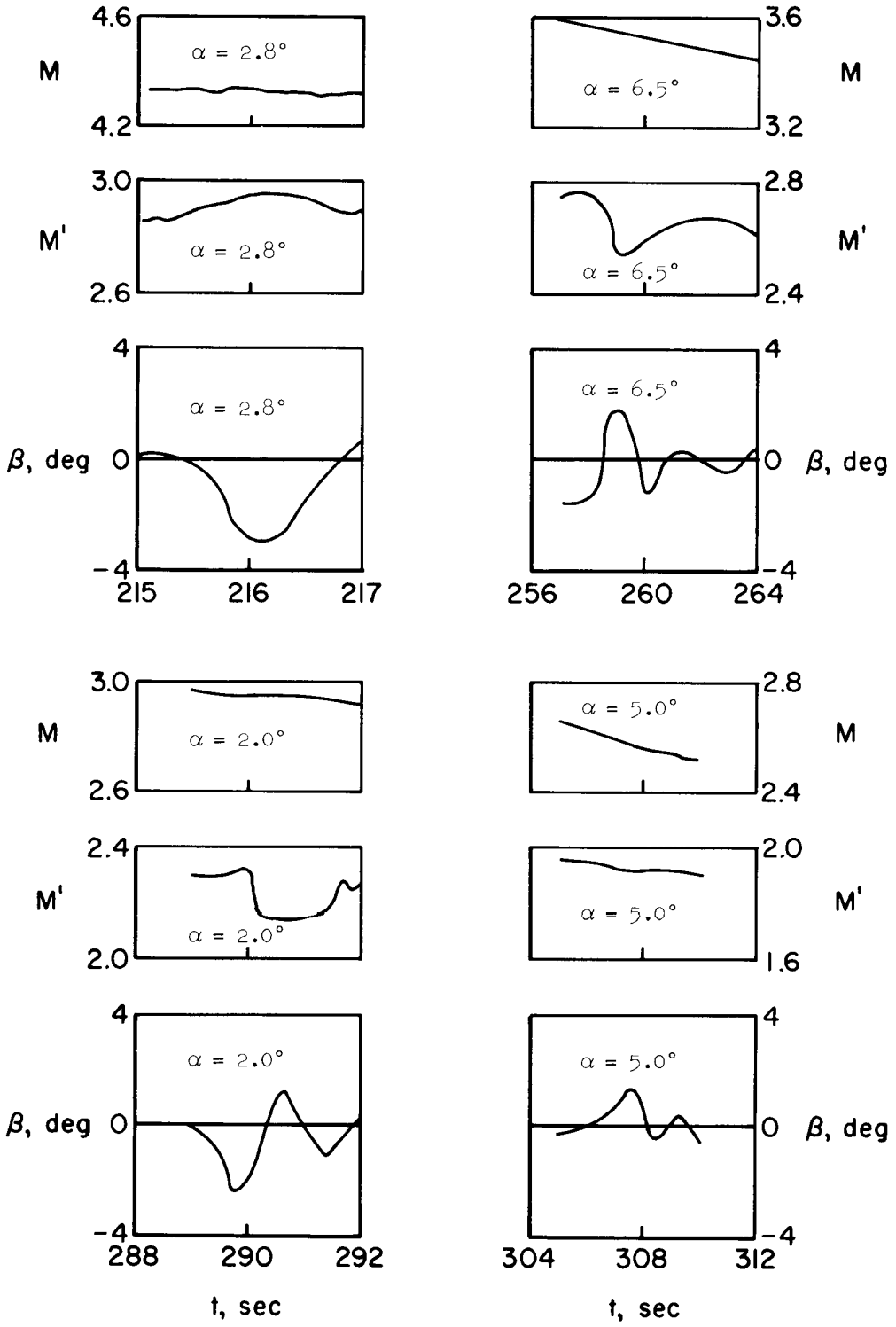

Figure 14.- Flush static position errors evidenced during oscillatory sideslip variations.

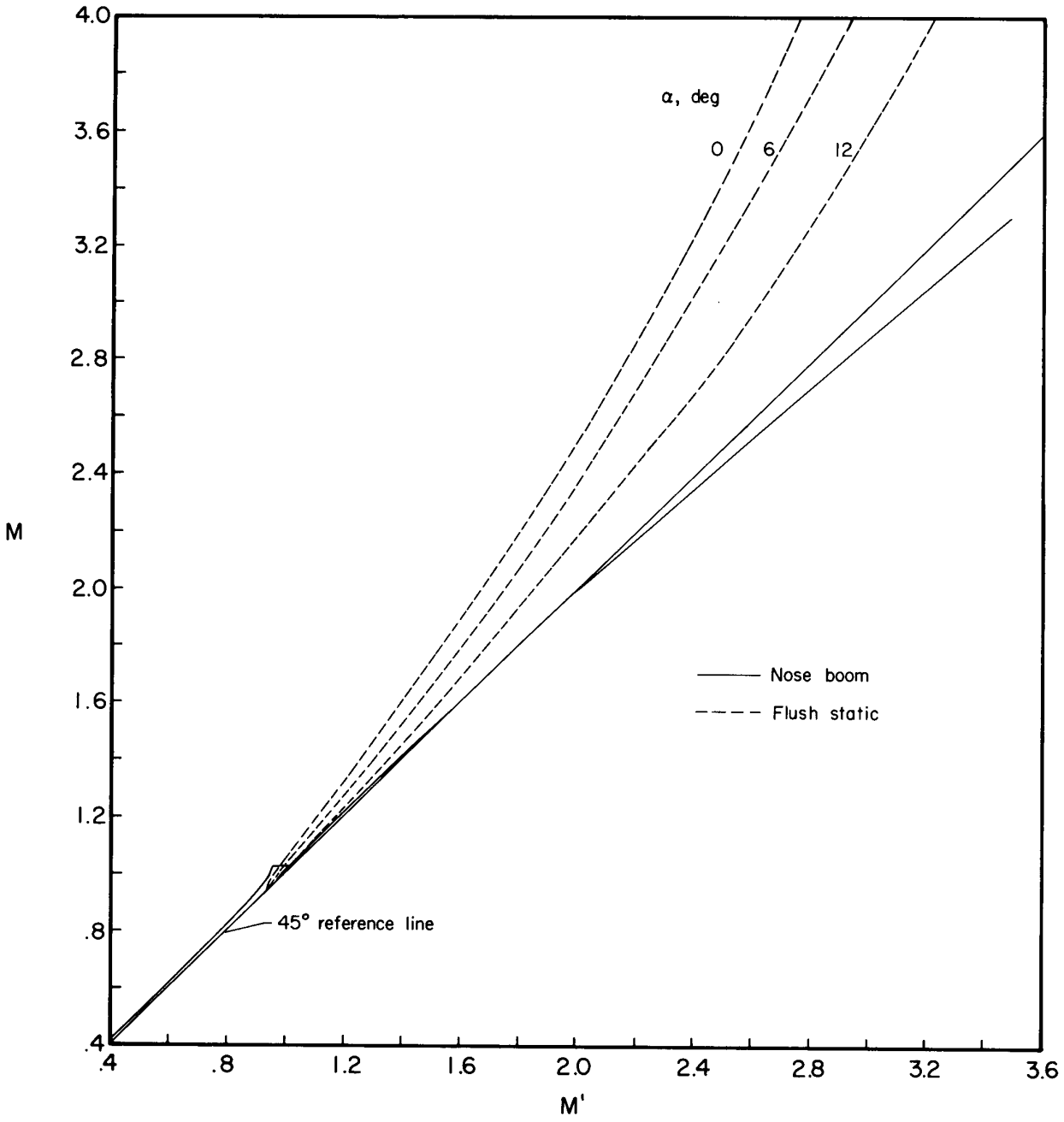

(a) Mach number.

Figure 15.- Comparison of the position-error calibrations for the nose-boom and flush static (ball nose) systems.

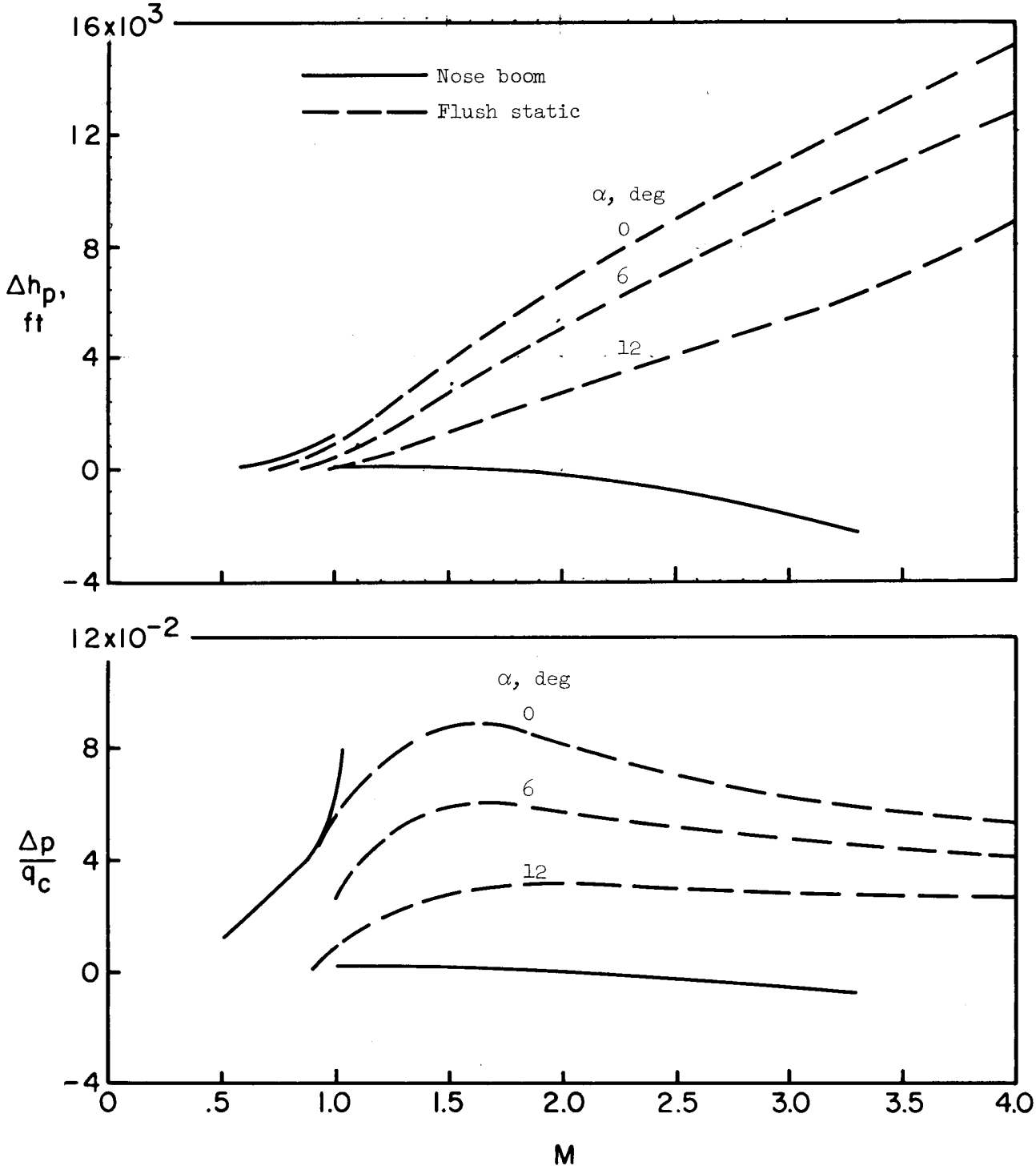

(b) Altitude and static pressure.

Figure 15.- Concluded.

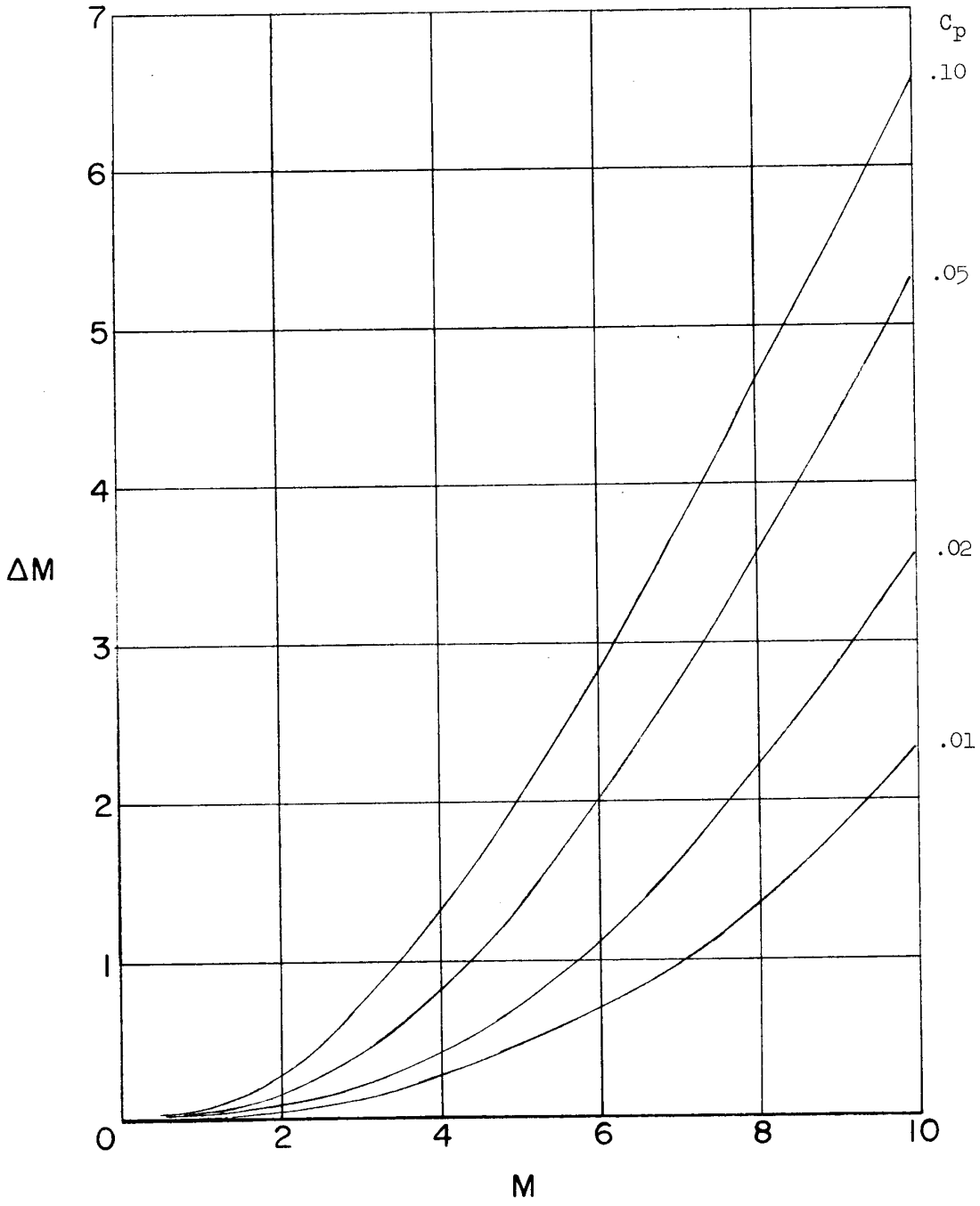

Figure 16.- Mach number errors associated with various values of static-pressure coefficient.

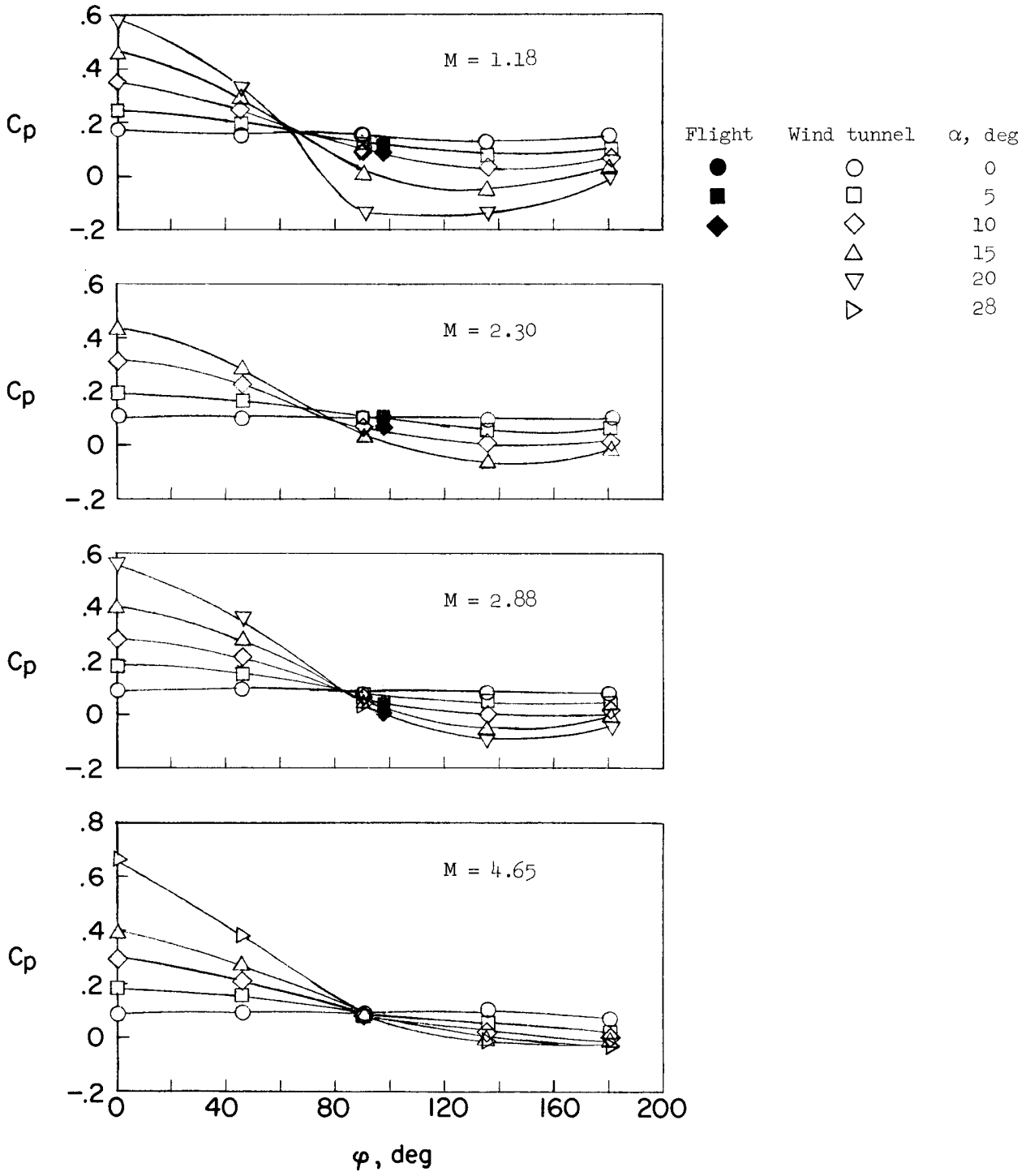

Figure 17.- Variation of static-pressure coefficient with fuselage meridian angle for various Mach numbers and angles of attack at station 50. No surface-control deflections; speed brakes closed; $\beta = 0°$.

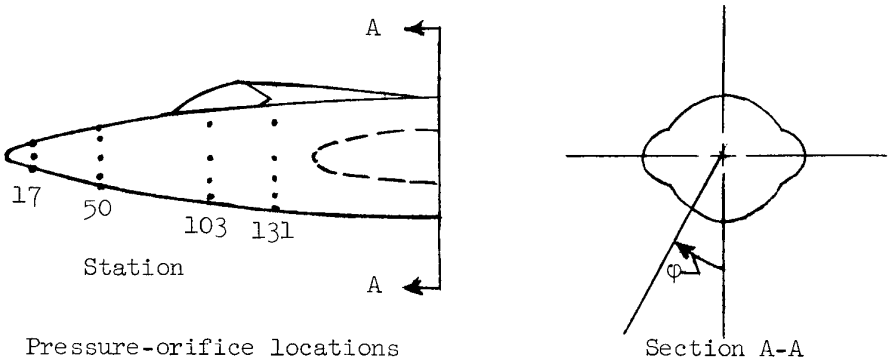

Pressure-orifice locations
(refs. 26,27)

Section A-A

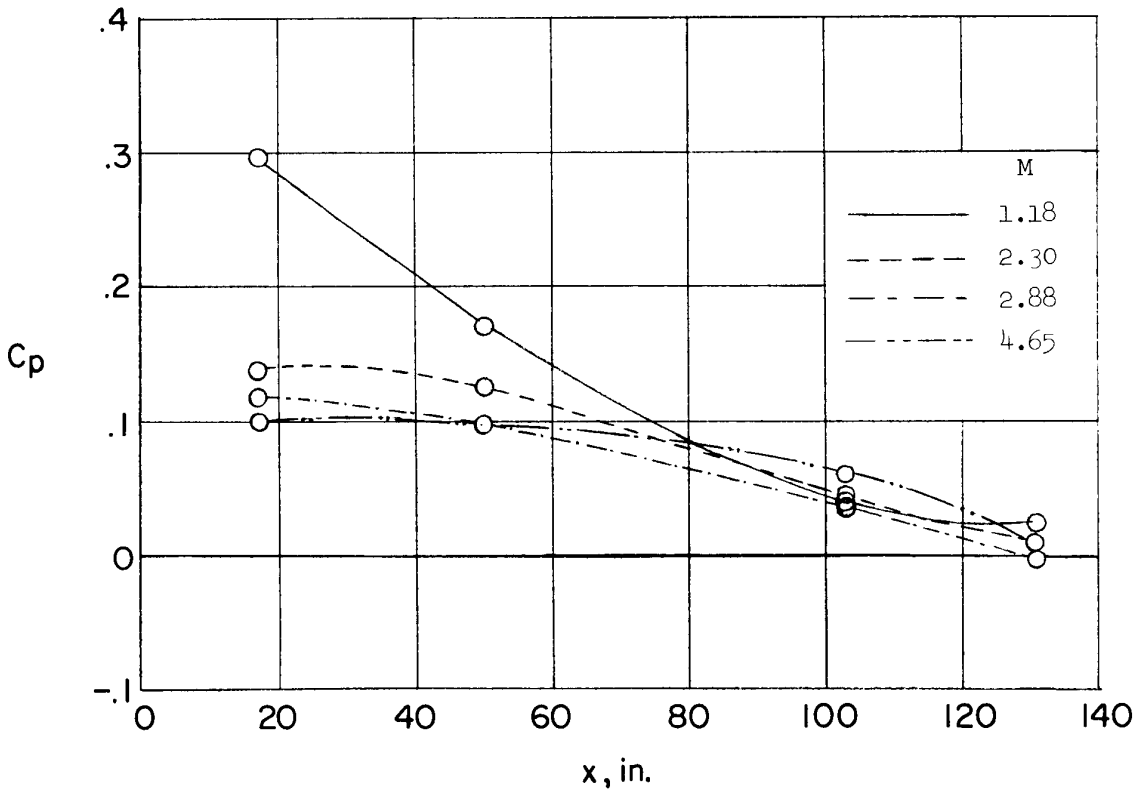

Figure 18.- Variation of mean pressure coefficient with X-15 fuselage station for circumferential fuselage locations corresponding to minimum static-pressure sensitivity to angle of attack. No control-surface deflections; speed brakes closed; $\beta = 0°$.

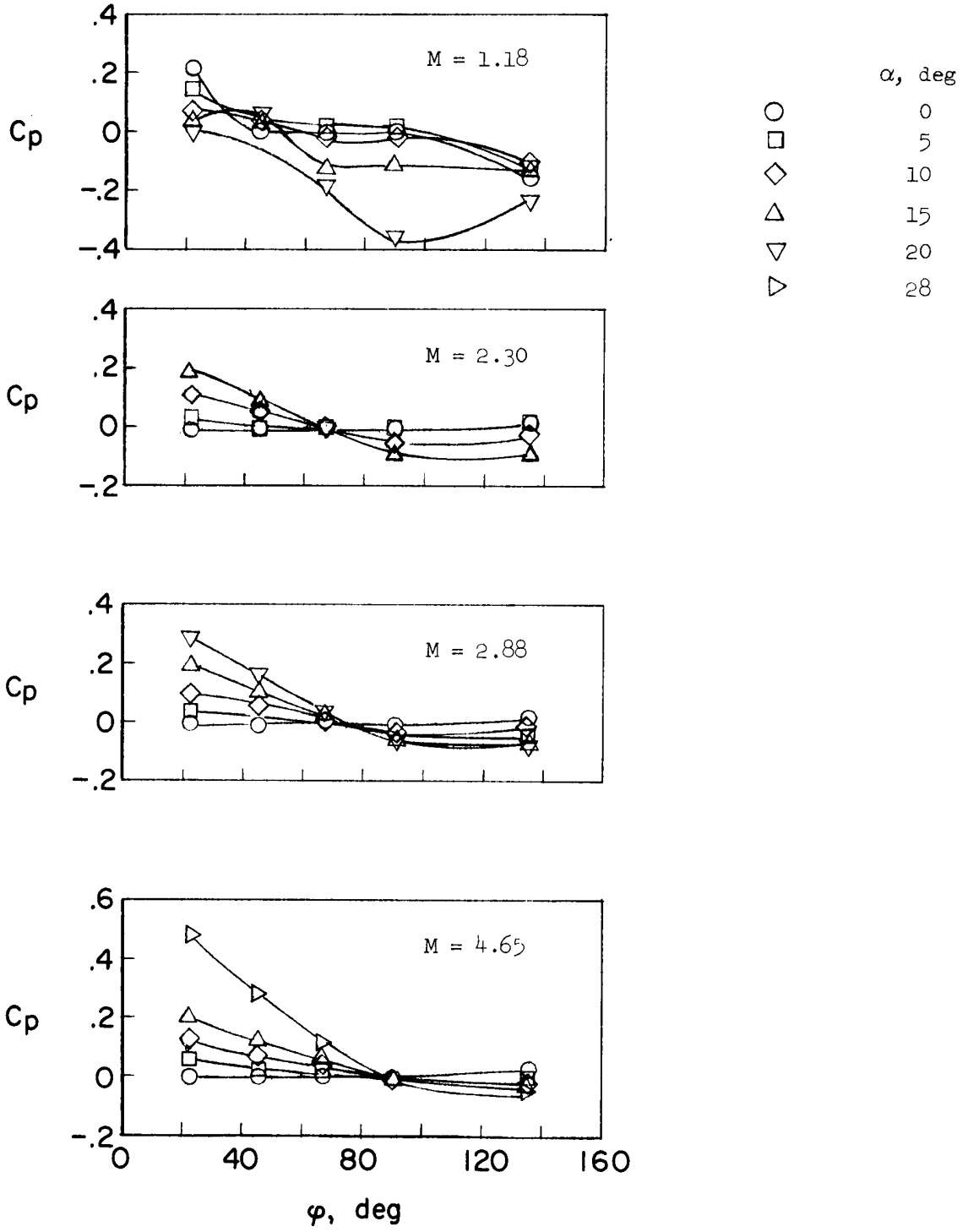

Figure 19.- Variation of static-pressure coefficient with fuselage meridian angle for various Mach numbers and angles of attack at station 131 as determined in wind-tunnel tests.

NASA TN D-1724
National Aeronautics and Space Administration.
CALIBRATIONS AND COMPARISONS OF PRESSURE-TYPE AIRSPEED-ALTITUDE SYSTEMS OF THE X-15 AIRPLANE FROM SUBSONIC TO HIGH SUPERSONIC SPEEDS. Terry J. Larson and Lannie D. Webb. February 1963. 36p. OTS price, $1.00. (NASA TECHNICAL NOTE D-1724)

X-15 flight calibration data to define static-pressure position errors are presented for two types of pressure-sensing configurations: a standard NACA pitot-static tube attached to a nose boom, and two manifolded flush static-pressure ports on the ogive nose. The position-error calibrations are presented up to M = 3.31 for the standard nose-boom installation and to M = 4 for the flush static system. Presented also are stagnation-pressure errors sensed by a pitot probe ahead of the canopy. Methods used to determine the position errors are described. The nose-boom configuration is shown to be superior from the standpoint of position error and ease of calibration for the available data range.

I. Larson, Terry J.
II. Webb, Lannie D.
III. NASA TN D-1724

NASA

NASA TN D-1724
National Aeronautics and Space Administration.
CALIBRATIONS AND COMPARISONS OF PRESSURE-TYPE AIRSPEED-ALTITUDE SYSTEMS OF THE X-15 AIRPLANE FROM SUBSONIC TO HIGH SUPERSONIC SPEEDS. Terry J. Larson and Lannie D. Webb. February 1963. 36p. OTS price, $1.00. (NASA TECHNICAL NOTE D-1724)

X-15 flight calibration data to define static-pressure position errors are presented for two types of pressure-sensing configurations: a standard NACA pitot-static tube attached to a nose boom, and two manifolded flush static-pressure ports on the ogive nose. The position-error calibrations are presented up to M = 3.31 for the standard nose-boom installation and to M = 4 for the flush static system. Presented also are stagnation-pressure errors sensed by a pitot probe ahead of the canopy. Methods used to determine the position errors are described. The nose-boom configuration is shown to be superior from the standpoint of position error and ease of calibration for the available data range.

I. Larson, Terry J.
II. Webb, Lannie D.
III. NASA TN D-1724

NASA

NASA TN D-1724
National Aeronautics and Space Administration.
CALIBRATIONS AND COMPARISONS OF PRESSURE-TYPE AIRSPEED-ALTITUDE SYSTEMS OF THE X-15 AIRPLANE FROM SUBSONIC TO HIGH SUPERSONIC SPEEDS. Terry J. Larson and Lannie D. Webb. February 1963. 36p. OTS price, $1.00. (NASA TECHNICAL NOTE D-1724)

X-15 flight calibration data to define static-pressure position errors are presented for two types of pressure-sensing configurations: a standard NACA pitot-static tube attached to a nose boom, and two manifolded flush static-pressure ports on the ogive nose. The position-error calibrations are presented up to M = 3.31 for the standard nose-boom installation and to M = 4 for the flush static system. Presented also are stagnation-pressure errors sensed by a pitot probe ahead of the canopy. Methods used to determine the position errors are described. The nose-boom configuration is shown to be superior from the standpoint of position error and ease of calibration for the available data range.

I. Larson, Terry J.
II. Webb, Lannie D.
III. NASA TN D-1724

NASA

NASA TN D-1724
National Aeronautics and Space Administration.
CALIBRATIONS AND COMPARISONS OF PRESSURE-TYPE AIRSPEED-ALTITUDE SYSTEMS OF THE X-15 AIRPLANE FROM SUBSONIC TO HIGH SUPERSONIC SPEEDS. Terry J. Larson and Lannie D. Webb. February 1963. 36p. OTS price, $1.00. (NASA TECHNICAL NOTE D-1724)

X-15 flight calibration data to define static-pressure position errors are presented for two types of pressure-sensing configurations: a standard NACA pitot-static tube attached to a nose boom, and two manifolded flush static-pressure ports on the ogive nose. The position-error calibrations are presented up to M = 3.31 for the standard nose-boom installation and to M = 4 for the flush static system. Presented also are stagnation-pressure errors sensed by a pitot probe ahead of the canopy. Methods used to determine the position errors are described. The nose-boom configuration is shown to be superior from the standpoint of position error and ease of calibration for the available data range.

I. Larson, Terry J.
II. Webb, Lannie D.
III. NASA TN D-1724

NASA